Universität Rostock

Traditio et Innovatio

Role of HCN Channels in Regulation of Synaptic Plasticity at Early Postnatal Medial Perforant Path

Dissertation

to obtain the academic degree of

Doctor of Human Sciences

(doctor rerum humanarum)

at Faculty of Medicine

Institute of Physiology

University of Rostock

Rostock, 2013

Submitted by:

Badel Gulshat (Guli Xiati)

from China

Born 05.05.1985. Xinjiang, China

Abstract

Hyperpolarization-activated, cyclic nucleotide-gated nonselective (HCN) channels modulate both membrane potential and resistance and play a significant role in synaptic plasticity. We compared the influence of HCN channels on long-term depression (LTD) at the medial perforant path-granule cell synapse in early postnatal (P9–15) and adult (P30–60) rats. LTD was elicited in P9–15 slices using low-frequency stimulation (LFS, 900 pulses, 1Hz; 80 ± 4% of baseline). Application of the specific HCN channel blocker ZD7288 (10 µM) before LFS significantly enhanced LTD (62 ± 4%; P < 0.01), showing HCN channels restrain LTD induction. However, when ZD7288 was applied after LFS, LTD was similar to control values and significantly different from the values obtained with ZD7288 application before LFS (81 ± 5%; P < 0.01), indicating that HCN channels do not modulate LTD expression. LTD in slices from adult rats were only marginally lower compared to those in P9–15 slices (85 ± 6%), but bath application of ZD7288 prior to LFS resulted in the same amount of LTD (85 ± 5%). HCN channels in adult tissue hence lose their modulatory effect. In conclusion, we found that HCN channels at the medial perforant path-granule cell synapse compromise LFS-associated induction, but not expression of LTD in early postnatal, but not in adult, rats.

Contents

3.   Results

4.   Discussion

5.   Reference

Abbreviation

1. AC — Associational Commisural pathway

2. ACSF — Artificial cerebrospinal fluid

3. AMPAR — α-amino-3-hydroxy-5-methyl-4-isoxazolepropionic acid receptor

4. APV — DL-2-amino-5-phosphonovalerate

5. CA — Cornu ammonis

6. CA 1-4 — Cornu Ammonis 1-4 region

7. CaM — Calmodulin

8. Ca^{2+}/CaM — Ca2+/Calmodulin

9. cAMP — Cyclic adenosine monophosphate

10. cGMP — Cyclic guanosine monophosphate

11. CNBD — Cyclic nucleotid binding domain

12. CNS — Central nervous system

13. D-AP5 — D-2-amino-5-phosphonopentanoate

14. DG — Dentate gyrus

15. EC — Entorhinal cortex

16. EGTA — Ethylene glycol-bis(2-aminoethylether)-N,N,N′,N′-tetraacetic acid

17. eNOS — Endothelial Nitric oxide synthase

18. EPSP — Excitatory post-synaptic potential

19. fEPSPs — Field excitatory postsynaptic potentials

20. GC — Guanylate cyclase

21. GluN1 — N-methyl-D-aspartate receptor subunit 1

22. HB — Hippocampal Body

23. HH — Head of the Hippocampus

24.	HCN	Hyperpolarization-activated cylic nucleotide gated nonselective cation channel
25.	HT	Hippocampal Tail
26.	I_f	Funny current
27.	I_h	Hyperpolarization-activated cation currents
28.	KAR	Kainate receptor
29.	LFS	Low frequency stimulation
30.	L-NAME	NG-Nitro-L-arginine methyl ester hydrochloride
31.	LPP	Lateral perforant pathway
32.	LTD	Long-term depression
33.	LTP	Long-term potentiation
34.	MF	Mossy fibers
35.	mGluR	Metabotropic Glutamate receptor
36.	MML	Middle molecular layer
37.	MPP	Medial perforant pathway
38.	NMDAR	N-methyl-D-aspartate receptor
39.	NO	Nitric oxide
40.	NO-GCs	Nitric oxide – sensitive guanylyl cyclases
41.	NOS	Nitric oxide synthase
42.	nNOS	Neuronal Nitric oxide synthase
43.	PIP2	Phosphatidylinositol 4,5-bisphosphate
44.	PKA	Protein Kinase A
45.	PP	Perforant path
46.	PP1	Protein Phosphatase 1
47.	PP2B	Protein Phosphatase 2B
48.	PPR	Paired-pulse ratio
49.	PSD95	Postsynaptic density protein 95

50. Sb   Subiculum

51. SC   Schaffer Collateral pathway

52. TS   Terminal Segment of the hippocampal tail

53. ZD7288   4-Ethylphenylamino-1,2-dimethyl-6-
methylaminopyrimidinium chloride

List of Tables and Figures

1. Introduction

1.1. Hippocampus

1.1.1. Anatomy of the hippocampus

The hippocampus is a major component of the brain. It belongs to the limbic system and plays a main role in the formation of episodic memories in humans (Aggleton and Brown, 1999;Reilly, 2001), spatial navigation and in consolidating information into long-term declarative memory (Mumby et al., 1999).

Throughout the head, body and tail, the hippocampus comprises two cortical layers rolled up inside one another (Figure 1). These layers can be seen to run from the head of the hippocampus throughout its body to its tail and form the two major cellular subfields: the cornu ammonis (CA) and the dentate gyrus (DG). The CA can be further sub-divided into four cellular regions or subfields (CA 1-4).
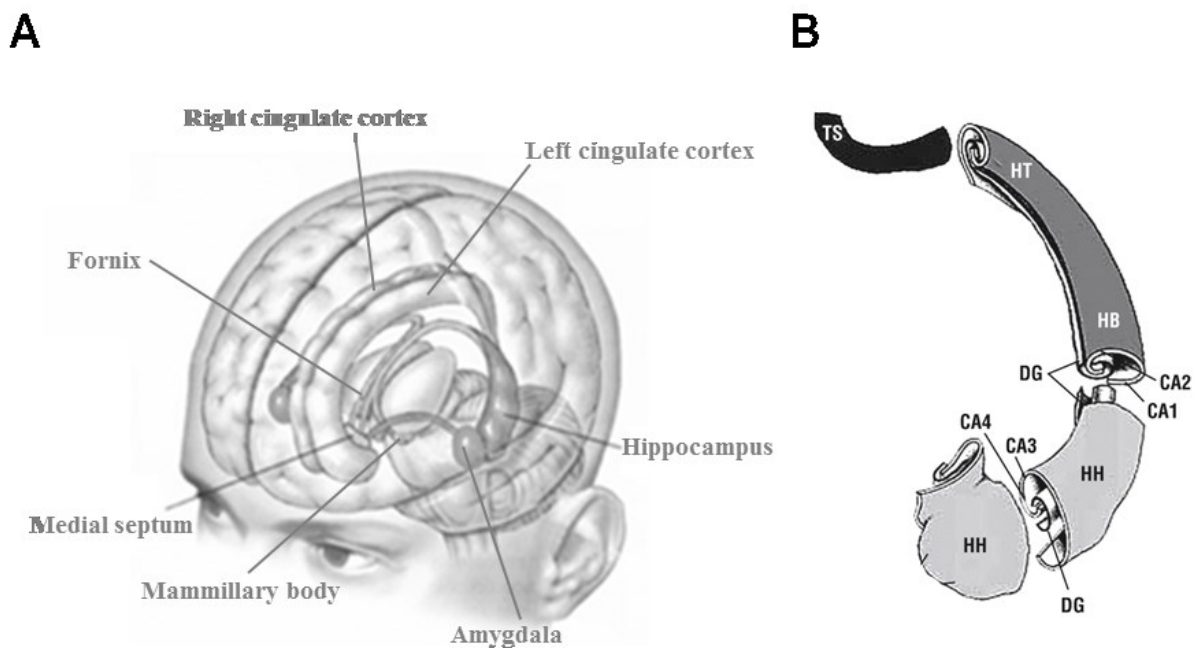
Figure 1: Location and subfield of the hippocampus

(A) The human brain, showing the location of the hippocampus and associated structures: Amygdala, mammillary body, the medial septum, fornix, the right and left cingulate cortex. **(B)** Components and subfields of the left hippocampus denote by the letters: Dentate Gyrus (DG), Cornu Ammonis 1-4 region (CA 1-4), Hippocampal Body (HB), Head of the Hippocampus (HH), Hippocampal Tail (HT), and Terminal Segment of the hippocampal tail (TS). This figure is modified from (Peterson et al., 2007).

The laminar organization of DG is the stratum moleculare layer, the stratum granulosum layer and the polymorph layer (or Hilus). The axons of the granule cells emerge close to the basal pole of the somata where it passes unmyelinated into the hilus and the CA3 hippocampus (Figure 2).

The intertwining apical dendrites of the granule cells and their afferents form the molecular layer. The molecular layer is thick and separated from the stratum molecular of the CA by the vestigial hippocampal sulcus. Its outer two-thirds receive fibers from the perforant pathway, while the inner third, in contact with the stratum granulosum, are occupied by commissural and septal fibers (Cerbone et al., 1993).
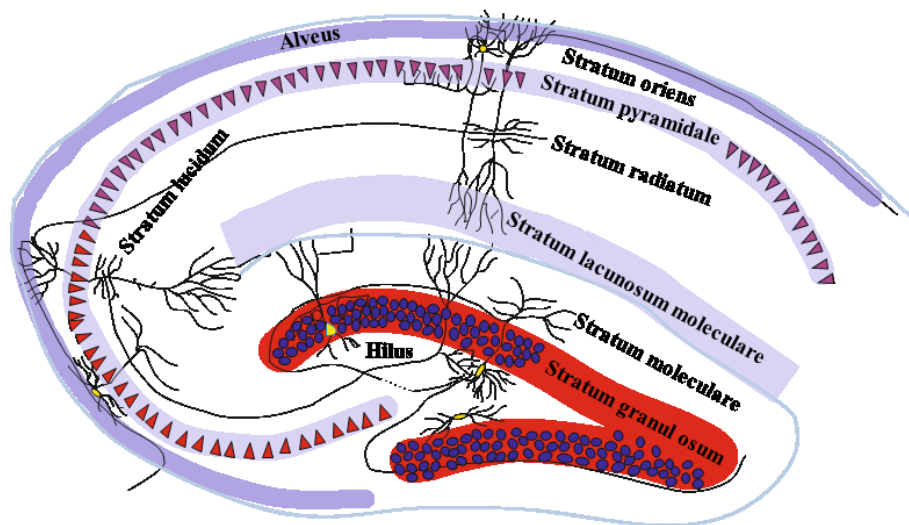
Figure 2: Internal structure of the hippocampus

The internal structure of the hippocampus, showing the laminar organization of the cornu ammonis (CA1-CA4) and the DG as viewed in the horizontal plane. CA: Alveus, Stratum oriens, Stratum pyramidale, Stratum radiatum/Stratum lucidum, and Stratum lacunosum moleculare. DG: Stratum moleculare, Stratum granulosum, and Hilus (polymorphic layer).

1.1.2. Hippocampal network

There are a variety of sources that contribute afferent fibers to the hippocampal formation. The entorhinal cortex (EC) is a major source of inputs to the hippocampus collecting information from the cingulate cortex, temporal lobe cortex, amygdala, orbital cortex, and olfactory bulb (Dolorfo and Amaral, 1998). Separate groups of fibers arising from the lateral and medial parts of the EC pass through the alveus and molecular layers of the hippocampus and DG respectively, to supply much of the hippocampus. The lateral pathway is called the lateral perforant pathway (LPP) and passes from the lateral entorhinal cortex into the molecular layer of the hippocampus. The medial pathway is called the medial perforant pathway (MPP) and enters the alveus of the hippocampus after passing through the white matter adjoining the subiculum.

The efferent connections of the hippocampal formation arise from pyramidal cells located in both the hippocampus and subicular cortex. The axons of these cells contribute the largest component to the fornix system of fibers.

The hippocampus coordinates information from a variety of sources. Information flows into the hippocampus mainly by the perforant path (PP) which targets neurons in the DG and in the CA1-3 regions as shown in Figure 3. The PP can be segregated into LPP and MPP, depending on whether the fibers arise from the lateral or medial entorhinal cortex. The axons of the PP arise principally in layers II and III of the ipsilateral EC, with minor contributions from the deeper layers IV and V. Axons from layers III/V project to the distal stratum lacunosum molecular layer of the CA1 and the molecular layer of the subiculum. Axons from layers II/VI densely project to the molecular layers of the DG and send a longer projection to CA3 which directly innervate the pyramidal cells of CA3. LPP generally project to the outer layers of the DG, whereas MPP terminate in deeper regions of the DG. The DG connects CA3 by the mossy fiber pathway. The mossy fibers (MFs) directly project to the stratum lucidum of the CA3. From the CA3 neurons, the signal leaves via the Schaffer collateral fibers which innervate the pyramidal cells of CA1 and the commissural fibers which innervate the contralateral hippocampus. The pathway from CA1 to subiculum (Sb) and on to the EC forms the principal output from the hippocampus.
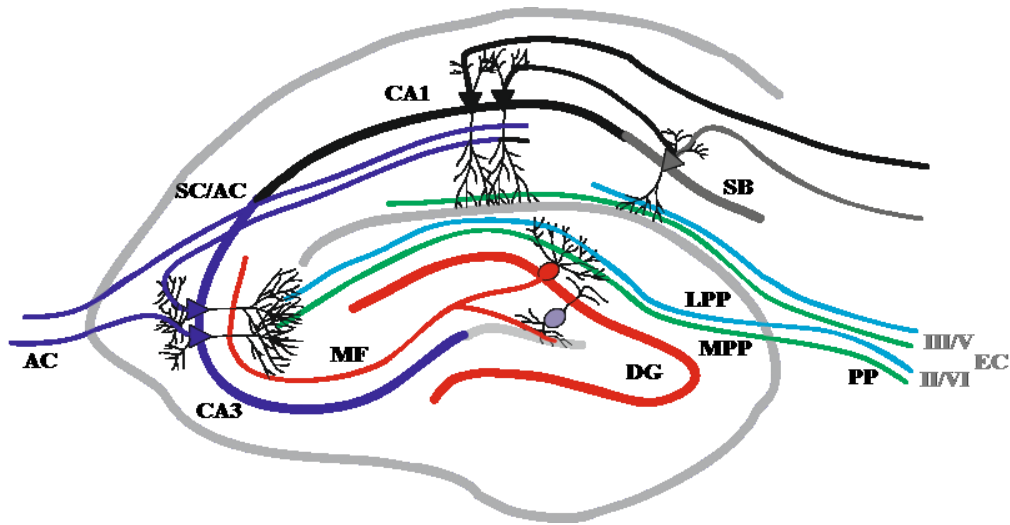
Figure 3: Hippocampal Network

The hippocampus forms a principally uni-directional network, with input from the Entorhinal Cortex (EC) that forms connections with the Dentate Gyrus (DG) and CA3 pyramidal neurons via the Perforant Path (PP), which split into lateral (LPP) and medial (MPP). CA3 neurons also receive input from the DG via the Mossy Fibres (MF). They send axons to CA1 pyramidal cells via the Schaffer Collateral Pathway (SC), as well as to CA1 cells in the contralateral hippocampus via the Associational Commisural (AC) pathway. CA1 neurons also receive inputs direct from the PP and send axons to the Subiculum (Sb). These neurons in turn send the main hippocampal output back to the EC, forming a loop.

1.1.3. Memory function of the hippocampus

Although it had historical precursors, function of hippocampus in memory derived its main impetus from a famous report by Scoville and Milner (Scoville and Milner, 1957) describing the results of surgical destruction of the hippocampus. The unexpected outcome of the surgery was severe anterograde and partial retrograde amnesia. In the ensuing years, patients with similar levels of hippocampal damage and amnesia have been studied as well, and thousands of experiments have studied the physiology of activity-driven changes in synaptic connections in the hippocampus. There is now almost universal agreement that the hippocampus plays an important role in memory; however, the precise nature of this role remains widely debated.

How learning and memory is achieved in the brain? Key to today's research into information storage in the brain is the concept of synaptic plasticity, a notion that has been heavily influenced by Hebb's (1949) postulate. Hebb conjectured that repeatedly and persistently co-active cells should increase connective strength among populations of interconnected neurons as a means of storing a memory trace. Since that time, strong support for his theory has been gained through a number of lines of research. Most important in this regard is likely the discovery of synaptic long-term potentiation (LTP) and long-term depression (LTD) within the mammalian hippocampus (Bear and Abraham, 1996;Bliss and Collingridge, 1993;Bliss and Lomo, 1973;Dudek and Bear, 1992;Lynch et al., 1977;Malenka and Nicoll, 1999). Intense interest has focused on these forms of synaptic plasticity (Abraham et al., 1994;Abraham, 2003;Doyere et al., 1997;Malenka and Bear, 2004;Staubli and Lynch, 1987) as they have a number of properties that make them suitable as models for the synaptic changes that likely occur during learning and memory (Doyere et al., 1993;Kemp and Manahan-Vaughan, 2007). Since the discovery of LTP and LTD, rigorous experiments have been conducted to search the mechanisms underlying them. It is generally well accepted that the induction and expression of LTP and LTD depend on the activation of synaptic transmissions (Mcentee and Crook, 1993).

1.2. Synaptic plasticity

1.2.1. Historical discovery of synaptic plasticity

In 1973, Terje Lømo and Tim Bliss first described the now widely studied phenomenon of long-term potentiation (LTP) on the synapse between the perforant path and dentate gyrus in the hippocampi of anaesthetised rabbits (Bliss and Lomo, 1973;Lomo, 2003). They were able to show a burst of tetanic (100 Hz) stimulus on perforant path fibers led to a dramatic and long-lasting augmentation in the postsynaptic response of cells onto which these fibers synapse in the dentate gyrus. This discovery generated interest due to the proposed role of the hippocampus in certain forms of memory. LTP in the hippocampus has been widely studied since it is believed that the mechanisms involved in its induction, expression, and maintenance are fundamental to learning and memory (Bliss and Collingridge, 1993). LTP is observed as a sustained increase in synaptic efficacy while LTD is a sustained decrease in synaptic efficacy. In 1977, Lynch and colleagues first observed heterosynaptic depression in which a reversible reduction of synaptic response in a nonstimulated pathway resulted after inducing LTP in a separate pathway in the CA1 region in vitro (Lynch et al., 1977). Levy and Steward also observed heterosynaptic LTD in vivo in the dentate gyrus indicating that the phenomenon could be applied to different brain areas (Levy and Steward, 1979). More and more paradigms have been tested and revealed various phenomena concerning synaptic plasticity in the hippocampus (Bashir and Collingridge, 1994;Calabresi et al., 1992;Dudek and Bear, 1992;Fujii et al., 1991;O'Dell and Kandel, 1994;Staubli and Lynch, 1990;Wang and Gean, 1999;Ziakopoulos et al., 1999) but also in other parts of the brain (Calabresi et al., 1992;Wang and Gean, 1999;Ziakopoulos et al., 1999).

Then scientists began to investigate the functional significance of LTP and LTD by using selective antagonists of those excitatory amino acid receptors whose activation is essential for their induction. In 1983, Lynch and colleagues reported that intracellular injections of the calcium chelator N,N,N',N'-tetraacetic acid (EGTA) block the development of hippocampal LTP (Lynch et al., 1983). At the same time Collingridge and colleagues discovered application of the selective NMDA receptor antagonist, DL-2-amino-5-phosphonovalerate (APV) had no effect on the excitatory post-synaptic potential (EPSP), but blocks LTP of synaptic transmission evoked by high frequency stimulation of the Schaffer collateral-commissural pathway (Collingridge et al., 1983). In 1992, it was reported that LTD is also synapse specific, and required activation of post-synaptic NMDA receptors as well (Dudek and Bear, 1992;Lee et al., 1998;Mulkey and Malenka, 1992). These results strongly suggested that hippocampal LTP and LTD are NMDA receptor dependent processes.

1.2.2. Mechanisms of Long term depression

Long-term depression in the CNS has been the subject of intense investigation as a process that may be involved in learning and memory and in various pathological conditions. Homosynaptic LTD has been first induced by low frequency stimulation (LFS) at 1 Hz in the CA1 area of the rat hippocampus (Dudek and Bear, 1992). This form of LTD has been shown to be NMDA receptor dependent (Dudek and Bear, 1992). Subsequently, NMDA receptor independent forms of LTD have been reported (Kobayashi et al., 1997;Oliet et al., 1997;Omara et al., 1995b;Wang et al., 1997).

Most synapses that undergo LTD use L-glutamate as their neurotransmitter. L-glutamate acts on N-methyl-D-aspartate receptor (NMDAR), α-amino-3-hydroxy-5-methyl-4-isoxazolepropionic acid receptor (AMPAR), kainate receptor (KAR) and metabotropic glutamate receptor (mGluR)2 (Hollmann et al., 1989;Hollmann and Heinemann, 1994;Lodge, 2009). Amongst two kinds of excitatory receptors involved in plasticity that have undergone extensive research are NMDAR and AMPAR (Mayer and Armstrong, 2004).

AMPAR requires glutamate binding to activate, allowing Na^+ flow into the neuron and causing an excitatory postsynaptic potential. NMDARs are usually composed of two GluN1 subunits and two GluN2 subunits, although GluN3 subunits sometimes replace GluN2 (Cull-Candy et al., 2001;Paoletti and Neyton, 2007). The two GluN2 subunits can be identical (GluN2A, GluN2B, GluN2C or GluN2D), forming a diheteromer, or they can be different from each other, forming a triheteromer together with two identical GluN1 subunits. The NMDAR requires both ligand (glutamate together with the co-agonist glycine or D-serine) and voltage activation (Kleckner and Dingledine, 1988;Laube et al., 1998;Wolosker, 2006). Under conditions of low post-synaptic activity, NMDARs are blocked in a voltage-dependent manner by extracellular Mg^{2+} ions (Johnson and Ascher, 1990). When post-synaptic activity is high, such as under conditions suitable for producing plasticity, the post-synaptic membrane depolarizes enough to remove the magnesium block (Cull-Candy et al., 2001;Dingledine et al., 1999;Paoletti and Neyton, 2007). Once activated, NMDARs are also highly permeable to calcium ions (Crowder et al., 1987). While both receptors lead to depolarization, NMDAR also brings about intracellular calcium ion concentration changes. Postsynaptic free Ca^{2+} are very important in calcium dependent second messengers and pathways, which are involved in synaptic plasticity (Malenka and Bear, 2004). Activation of NMDA receptors increases postsynaptic free Ca^{2+}, which is thought to stimulate the release of calmodulin (CaM), a calcium-binding activator protein found mainly in the brain and heart.

LTD induction depends on intracellular calcium elevation. The relative change in intracellular calcium concentration determines whether LTP or LTD is induced (Cummings et al., 1996). The rise in postsynaptic calcium can result from calcium influx mainly through NMDA receptors and/or voltage gated calcium channels and/or calcium release from intracellular stores (Christie et al., 1996;Kobayashi et al.,

1997;Mulkey and Malenka, 1992;Omara et al., 1995a;Wang et al., 1997) which initiate LTD by leading to several second messenger related cellular responses. LTD arises from activation of calcium-dependent phosphatases that dephosphorylate the target proteins (Mulkey et al., 1993). In particular the calcineurin (PP2B), a Ca^{2+}/calmodulin(Ca^{2+} / CaM)-dependent protein phosphatase, dephosphorylates and inactivates inhibitor-1 (Mulkey et al., 1993;Mulkey et al., 1994). Inhibitor-1 is normally bound to postsynaptic serine/threonine protein phosphatase 1 (PP1). Inactivation of inhibitor-1 will release PP1 to dephosphorylate its substrates in the following. One of the substrates of PP1 is AMPA receptors (Lee et al., 2000). After LTD induction AMPA receptors are dephosphorylated at the PKA site (ser-845) and rapidly internalized (Carroll et al., 1999;Ehlers, 2000). Although various mechanisms may underlie the decrease in sensitivity to L-glutamate, the reduction in the number of postsynaptic AMPA receptors is the major expression mechanism for LTD (Malinow and Malenka, 2002).

In addition, LTD can also involve a reduction in the probability of glutamate release (Enoki et al., 2009;Feinmark et al., 2003;Stanton et al., 2003). This could be triggered by changes in the presynaptic terminal or by postsynaptic changes that are communicated across the synapse via a retrograde messenger. Several retrograde messengers have been proposed to be involved in LTD, including nitric oxide (NO) in NMDAR dependent LTD (Stanton et al., 2003) and lipoxygenase metabolites in hippocampal mGluR-LTD (Feinmark et al., 2003).

1.3. HCN channels

1.3.1. HCN channels in the hippocampus

Hyperpolarization-activated cation currents, termed I_h, were first described in cells of the sinoatrial node of the heart (Pape, 1996;Robinson, 2003) and called funny current (or I_f) because of specific biophysical properties (Noma and Irisawa, 1976). Later, I_h current is also found in other tissues: in heart muscles, in the central and peripheral nervous system, in the sensory cells as well as in endocrine and exocrine cells (Robinson, 2003). In the CNS, the I_h current contributes to several physiological properties and functions such as "pacemaker" of some neurons, control of membrane potential and the integration of dendritic synaptic inputs.

Figure 4: Structure of HCN channels

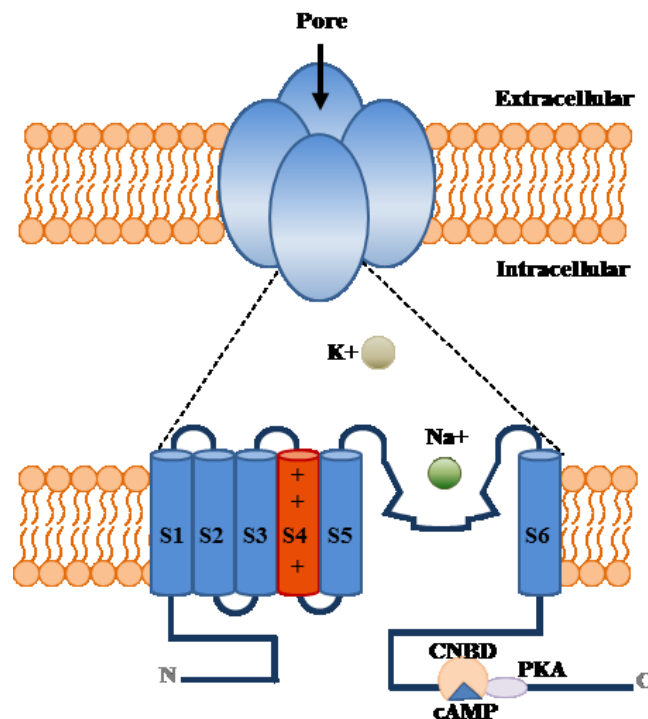HCN channels consist of four subunits composed of either identical or different HCN subunits. Each subunit contains six transmembrane domains (S1-S6) with the positively charged S4 functioning as the voltage sensor. The transmembrane segments S5 and S6 are connected via a pore loop carrying the ion selectivity filter. The C-terminus carries a cyclic nucleotide binding domain (CNBD) with PKA sites.

In mammals, four isoforms (HCN1-4) responsible for I_h currents encoding hyperpolarization-activated cyclic nucleotide gated channels (HCN channels) were cloned (Ludwig et al., 1998;Santoro and Tibbs, 1999). HCN channels are formed by the assembly of these four isoforms (Figure 4). The C-terminal region has an area sensitive to cyclic nucleotides-binding domain (CNBD) and a putative site for PKA phosphorylation in the CNBD (Monteggia et al., 2000). However, it is not clear how phosphorylation of these distal C-terminal sites affect the voltage dependence. This region could interact with other cytosolic domains, such as the CNBD or the transmembrane domains, and the voltage sensor directly. Binding of cyclic nucleotides (cAMP and / cGMP) facilitates channel opening, but binding of cyclic nucleotides is not sufficient to open the channels without an additional hyperpolarization of the membrane. HCN channels are cation nonselective allowing the passage of Na^+ and K^+. There is also evidence of minor permeation of Ca^{2+}.

HCN channels are abundantly distributed in the central nervous system (Gauss and Seifert, 2000;Magee, 1999;Pape, 1996;Santoro et al., 2000;Vasilyev and Barish, 2000;Williams and Stuart, 2000). In the hippocampus, subunits HCN1 and HCN2 are predominantly expressed (Monteggia et al., 2000;Notomi and Shigemoto, 2004). However, the expression of these isoforms is developmentally regulated (Bender et al., 2001;Bender et al., 2007;Brewster et al., 2007;Vasilyev and Barish, 2002), resulting in age-specific cellular complements of HCN channels and I_h properties (Surges et al., 2006;Vasilyev and Barish, 2002). These contribute to the generation of age-specific patterns of neuronal activity (Agmon and Wells, 2003;Bender et al., 2005). Neuronal activity, in turn, selectively modulates the expression of specific HCN channel isoforms (Brewster et al., 2002;Brewster et al., 2005;Santoro and Baram, 2003), thus governing the properties of I_h and, consequently, the excitability of hippocampal neurons (Chen et al., 2001).

Emerging evidence, though, suggests that in addition to their dendritic localization, HCN1 channels may be present on certain axons and synaptic terminals in the hippocampus, cortex and other regions of the brain (Bender et al., 2007;Lujan et al., 2005;Notomi and Shigemoto, 2004). It was initially reported that channels of the HCN1 subunits were expressed in the termination zone of perforant path fibers in the dentate gyrus of immature rats (Bender et al., 2007). Fine-structural analysis and disconnection studies revealed a presynaptic localization of these channels that was further supported by electrophysiological approaches demonstrating a contribution of I_h to the firing properties of the immature perforant path (Wilkars et al., 2012). Presynaptic HCN channels are expressed on glutamatergic axon terminals of the MPP input to dentate gyrus granule cells during the first 2-3 weeks of postnatal development, and subsequently are lost during maturation (Bender et al., 2007). These findings suggest that the axonal localization of HCN channels in the perforant path that occurs only during development. HCN1 mRNA and protein levels in the cells of origin in the entorhinal cortex did not decrease with age, whereas the expression of HCN channel molecules in axonal and presynaptic compartments was attenuated, suggesting that the transport of HCN1 channels to perforant path axons

changed with age. Further, blocking action potential firing increased presynaptic HCN1 channel expression, suggesting that network activity is involved in regulating axonal expression of the HCN1 channel.

1.3.2. Role of HCN channels in synaptic plasticity

HCN channels are low-threshold, voltage-gated ion channels with very unusual biophysical properties (Biel et al., 2009). These channels are open at potentials more negative to −50 mV and are important for regulating neuronal resting membrane potential. In addition, the channels are permeable to Na^+ and K^+ and form an inward current at rest, thereby depolarizing resting membrane potential. Interestingly, in the hippocampus and cortex, they are highly localized to pyramidal cell dendrites (Lorincz et al., 2002;Notomi and Shigemoto, 2004). By regulating the resting membrane potential and in this way the biophysical properties of other ion channels as well as by modulating the membrane resistance, they influence EPSP kinetics and integration (George et al., 2009;Huang et al., 2009;Magee, 1999;Tsay et al., 2007). These effects are likely to contribute substantially to synaptic plasticity and thus, process such as information storage (Brager and Johnston, 2007;Campanac et al., 2008;Fan et al., 2005;Nolan et al., 2004;Wang et al., 2007).

Since HCN channels are considerably open at the resting membrane potential and mediate a slowly inactivating and inwardly rectifying Na^+ current (Mccormick and Pape, 1990;Simeone et al., 2005), these channels appear to be ideal modulators of both the membrane potential and the membrane resistance of neurons, and thus may play a significant role in synaptic transmission.

In the recent years, it has become evident that HCN channels are also relevant modulators of synaptic plasticity (Bender et al., 2007;Mellor et al., 2002;Nolan et al., 2004;Tokay et al., 2009). Obviously, HCN channels may have differential effects on different synapses and/or various types of synaptic plasticity. While long-term potentiation (LTP) following electrical stimulation to the Schaffer collateral input of CA1 pyramidal cells was unaltered in HCN1-deficient mice, a significant enhancement of LTP was observed when the perforant path input to CA1 was stimulated (Nolan et al., 2004). Intriguingly, such a constraining role of HCN channels on synaptic plasticity in CA1 was also found with long-term depression (LTD) following pharmacological activation of group I metabotropic glutamate receptors (Tokay et al., 2009). However, LTD following electrical stimulation at the same synapse was also assessed and failed to be affected by HCN channel inhibition. In general, different induction and expression mechanisms on pre- and/or postsynaptic sites may be involved for multiple types of synaptic plasticity and at various synapses throughout the hippocampus, and hence may account for differential effects of HCN channels on synaptic plasticity. Thus, it is an intriguing task to unravel pre- and postsynaptic mechanisms of metaplasticity mediated by HCN channels.

1.4. Objective of the study

Previous reports from our lab and others pointed to a role of HCN channels in metabotropic glutamate receptor-dependent LTD (Tokay et al., 2009), but not in NMDAR-dependent LTP (Nolan et al., 2004), the central aim of this study was to investigate the role of presynaptic HCN channels on synaptic NMDAR-dependent LTD in the dentate gyrus. In this region, previous reports suggested the developmental down-regulation of HCN1 on presynaptic medial perforant path (MPP) terminals (Bender et al., 2007). Thus, comparison between early postnatal and adult tissue provides the unique opportunity to study the influence of HCN channels on LTD, since postsynaptic elements in this area hardly express HCN channels (Bender et al., 2007).

In the present study, following questions were addressed in detail:

1. Does HCN channel inhibition affect induction of LTD in early postnatal compared to adult animals?

2. Does HCN channel inhibition affect LTD levels after its induction?

3. Which presynaptic mechanisms may play a role?

2. Material and methods

2.1. Material

2.1.1. Animals

All experiments were performed with either early postnatal (P9–15) or adult (P30–60) male CD rats purchased from Charles River (Sulzfeld, Germany) and conformed to national and international guidelines on the ethical use of animals (European Council Directive 86/609/EEC).

2.1.2. Devices and software

Table 1: Devices

Designation	Manufacturer	Origin
Vibratome	Integraslice 7550MM, Campden Instruments, Loughborough	UK
Master-8 pulse stimulator	A.M.P.I., Jerusalem	Israel
Micro 1401 CED	Cambridge Electronic Design, Cambridge	England
Signal 2.16	Cambridge Electronic Design Ltd	England
EXT-08 (amplifier)	npi electronic GmbH	Germany
EXT-08-HS (preamplifier)	npi electronic GmbH	Germany
DPA-2FX (filter)	npi electronic GmbH	Germany
TC-10 Temperature Control	npi electronic GmbH, Tamm	U.S.A.
Stimulus Isolator A365	World Precision Instruments, Sarasota	U.S.A.
MZ 6 Stereo Zoom Mikroskope	Leica	Germany
KL 750 Kaltlichtquelle	Leica	Germany

LBM7 Manual Manipulator	Scientifica Ltd.	Germany
Interface Chamber	BSC-HT, Harvard Apparatus, Holliston	U.S.A.
Perimax - peristaltic pump	Spetec GmbH	Germany
Haake C10 Waterbath	Electron Corporation GmbH	Germany
Glass pipette	GB150-8P ,Science Products, Hofheim am Taunus	Germany
Pipette puller	PIP5, HEKA Elektronik, Lambrecht	Germany
Tefloninsulated platinum wires	PT-2T, Science Products	Germany
Silverwire	World Precision Instruments Inc.	U.S.A.
Platinwire isoliert 50 μm	Science Products GmbH	Germany
MC1 Analytic AC 120 S	Sartorius AG	Germany
Osmometer	Knauer	Germany
RET-GS Magnet stirrer	IKA Labortechnik GmbH	Germany
pH-Meter CG 840	Schott-Geräte GmbH	Germany

2.1.3. Chemicals and solutions

Table 2: Chemicals

Designation	Manufacturer	Origin
70% Ethanol	Carl Roth Ltd.	Germany
D-(+)-Glucose	Sigma Taufkirchen	Germany
Diethyl Ether	Mallinckrodt Baker, deventer	Netherlands
KCl	Sigma, Taufkirchen	Germany
$MgCl_2$	Sigma, Taufkirchen	Germany
$CaCl_2$	Sigma, Taufkirchen	Germany
$NaHCO_3$	Sigma, Taufkirchen	Germany
NaCl	Sigma, Taufkirchen	Germany
NaH_2PO_4	Sigma, Taufkirchen	Germany
NaOCl-solution, 13%	Applichem, Darmstadt	Germany
NaOH, 1 M	Merck, Darmstadt	Germany
HCl, rauchend 37%	Merck, Darmstadt	Germany
SR 95531 hydrobromide (Gabazine)	Tocris, Bristol	England
Saccharose	Sigma, Taufkirchen	Germany
ZD7288	Tocris, Bristol	England
L-NAME	Tocris, Bristol	England
D-AP5	Tocris, Bristol	England

The stock solutions of ZD7288 (50 mM), D-AP5 (100 mM), Gabazine (25 mM) and L-NAME (100 mM) were prepared with doubly distilled water. All stock solutions were stored at - 25 ° C until experimental use by bath application in ACSF.

Table 3: Dissection Solution for slice preparation

Chemical	Formula	Final concentration (mM)
Sodium Chloride	$NaCl$	125
Sodium Hydrogen Carbonate	$NaHCO_3$	26
Potassium Chloride	KCl	3
Sodium Hydrogen Phosphate	NaH_2PO_4	1.25
Calcium Chloride	$CaCl_2$	0.2
Magnesium Chloride	$MgCl_2$	5
Glucose	$C_6H_{12}O_6$	13

pH 7.4, osmolarity 326-328 mosmol / kg and stored up to one week at 4 ° C

Table 4: ACSF for electrophysiological recordings

Chemical	Formula	Final concentration (mM)
Sodium Chloride	$NaCl$	125
Sodium Hydrogen Carbonate	$NaHCO_3$	26
Potassium Chloride	KCl	3
Sodium Hydrogen Phosphate	NaH_2PO_4	1.25
Calcium Chloride	$CaCl_2$	2.5
Magnesium Chloride	$MgCl_2$	1.3
Glucose	$C_6H_{12}O_6$	13

pH 7.4, osmolarity 304-312 mosmol / kg and stored up to one week at 4 ° C

2.2. Methods

2.2.1. Hippocampal slice preparation

After deep anesthesia with diethyl ether, rats were decapitated with a guillotine. After removal of head, the occipital scalp was cut with scissors and split the skull and the dura mater with a median longitudinal section along the cerebral fissure. After the two halves of the skull were carefully worked out with tweezers aside, the cerebellum was removed with a spatula.

The remaining brain was rapidly submerged into oxygenated ice-cold dissection solution (Table 3; gassed with 95% O_2, 5% CO_2; pH 7.4) and fixed horizontally with superglue on the cutting model of the cutting chamber. This was then filled with ice-cold gassed preparation solution. Subsequently, horizontal brain slices (400 µm) of the hippocampus were prepared in this ice-cold dissection solution with a vibratome. The hippocampal formations of both hemispheres were carefully excised and then transferred into a holding chamber at room temperature filled with artificial cerebrospinal fluid (ACSF) (Table 4; gassed with 95% O_2, 5%CO_2; pH 7.4), where they remained at room temperature for at least 60 minutes, until they were then transferred into the interface chamber for recording.

2.2.2. Electrophysiology

For electrophysiological recordings, hippocampal slices were transferred into an interface chamber maintained at 32°C by means of a temperature controller and superfused with ACSF (composition as above, perfusion rate of 2- 3mL/min). Field excitatory postsynaptic potentials (fEPSPs) were recorded using borosilicate glass pipettes (GB150-8P) with a tip resistance of 2-3MΩ (fabricated with PIP5 puller) and filled with ACSF. Bipolar stimulating electrodes were made from Tefloninsulated platinum wires (PT-2T), and double-pulse stimulation (interstimulus interval 40ms) was delivered using a Master-8 stimulator and a stimulus isolator (A365) at a baseline rate of 0.033 Hz. The baseline stimulation strength was adjusted to 30–40% of the maximal fEPSP amplitude and typically in the range of 50–100 µA. The evoked potentials were amplified and filtered at 1 kHz by EXT-10-2F, digitized by Micro1401 (CED) and stored for off-line analysis by Signal 2.16.

To record from the medial perforant path–granule cell synapse, both the stimulating and the recording electrodes were placed into the middle molecular layer (MML) of the DG (Figure 5A). Since these synapses typically display paired-pulse depression (Figure 5B; (Dietrich et al., 1997;Kilbride et al., 1998) double-pulse stimulation (interstimulus interval of 40 ms) was used during the initial 5–7 minutes of each experiment, and the paired-pulse ratio (PPR) was calculated as the ratio of the 2nd pulse-evoked fEPSP to the 1st pulse-evoked fEPSP. In addition, gabazine (1 µM) was added to the ACSF in order to reduce contaminations by stimulation of local GABAergic interneuronal circuits, and single stimulation was used for the remaining experiment.
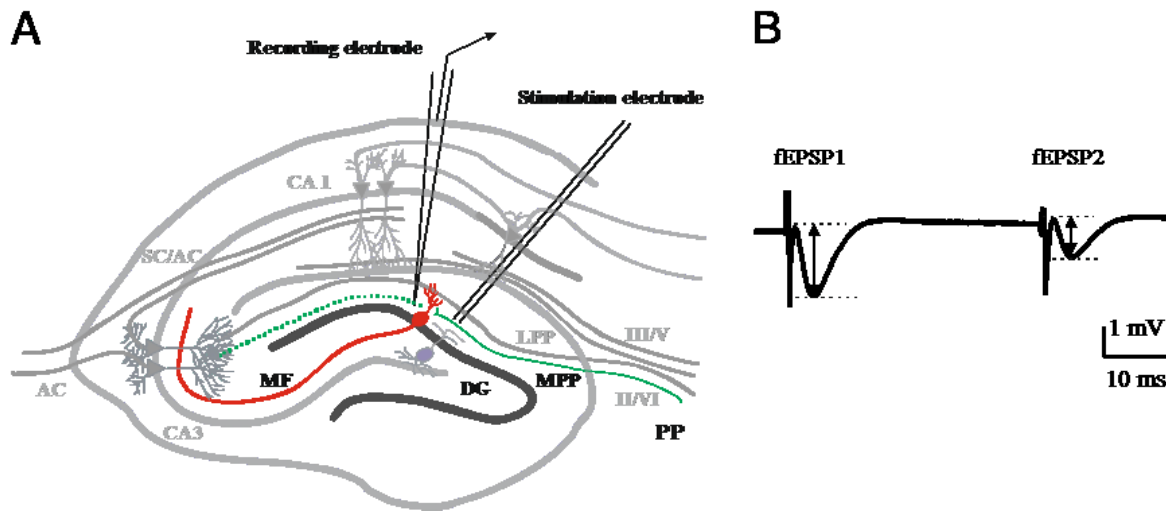
Figure 5: Schematic representation of extracellular recording of fEPSP

(A) Hippocampus slices with placement of stimulation and recording electrodes. **(B)** Double-pulse stimulation to MPP evokes a paired-pulse depression in synaptic responses. fEPSP amplitude is represented between the arrows.

Short-term depression (STD) and long-term depression (LTD) were induced by a low-frequency stimulation (LFS) protocol (as illustrated in Figure 6) consisting of 900-pulse-stimulation (at 1 Hz) for 15 min with baseline stimulation strength and 1.5- fold pulse width. STD is defined as the average of fEPSP amplitudes at 0–2min after LFS and LTD is defined as the average of fEPSP amplitudes at 55–60 minutes after LFS. Both STD and LTD values are given as fEPSP amplitudes expressed as the percentage of the baseline response. The influence of HCN channels and NO signaling pathways on LFS-induced LTD were tested by bath application of ZD7288 (10 μM) and L-NAME (100 μM), respectively, which were freshly dissolved in ACSF. Since ZD7288 was shown to depress glutamatergic receptors as well (Chen, 2004;Chevaleyre and Castillo, 2002), we performed interleaved experiments without LFS that were used to normalize the STD and LTD values. This normalization was performed by calculating the ratio of the LFS-treated by the non-LFS-treated control value and expressed as the percentage of baseline response. To test the NMDAR-dependence of LFS-LTD in MPP, the specific NMDA receptor antagonist D-2-amino-5-phosphonopentanoate (D-AP5, 50 μm) was applied prior to LFS.

900 Pulses @ 1 Hz
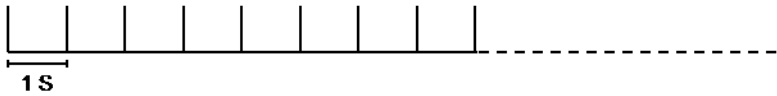
Figure 6: Schematic representation of low-frequency stimulation paradigm

Low-frequency stimulation paradigm used for LTD induction is consisting of 900 pulses at 1 Hz for 15 min.

2.2.3. Statistical Analysis

All data are expressed as means ± SEM the baseline fEPSP amplitude. Data were analyzed using Signal 2.6 software and the software Microsoft office excels 2010. Statistical comparisons were performed using Student's two-tailed t-test. Significant differences are indicated by asterisks ($*P < 0.05$; $**P < 0.01$; $***P < 0.001$) for comparisons between untreated and treated slices (unpaired test) and by open diamonds (◊ $P < 0.05$; ◊◊ $P < 0.01$) for comparisons between different time points within the same group (paired test).

3. Results

3.1. Influence of HCN channel blocker ZD7288 on LFS-induced LTD at MPP

3.1.1. LFS-induced LTD in early postnatal rats is enhanced by ZD7288

LTD in the hippocampus is commonly induced by LFS. An LFS protocol of 900 pulses at 1 Hz was employed in this study (indicated by an open bar in Figure 7A). Such a paradigm applied to the MPP input onto dentate gyrus-granule cells caused an immediate synaptic depression to 70 ± 6% of the baseline fEPSP amplitude (Figure 7A, closed symbols and Figure 7B, closed bar, n = 9). During the follow up of the experiment, this short-term depression (STD) resulted in stable LTD of 80 ± 4% of baseline at 60 minutes after LFS. Interleaved time-control experiments without LFS demonstrated that the recording conditions were stable for at least 90 minutes (100 ± 1% at the end of the experiment; open symbols in Figure 7A and open bar in Figure 7B, n = 12).
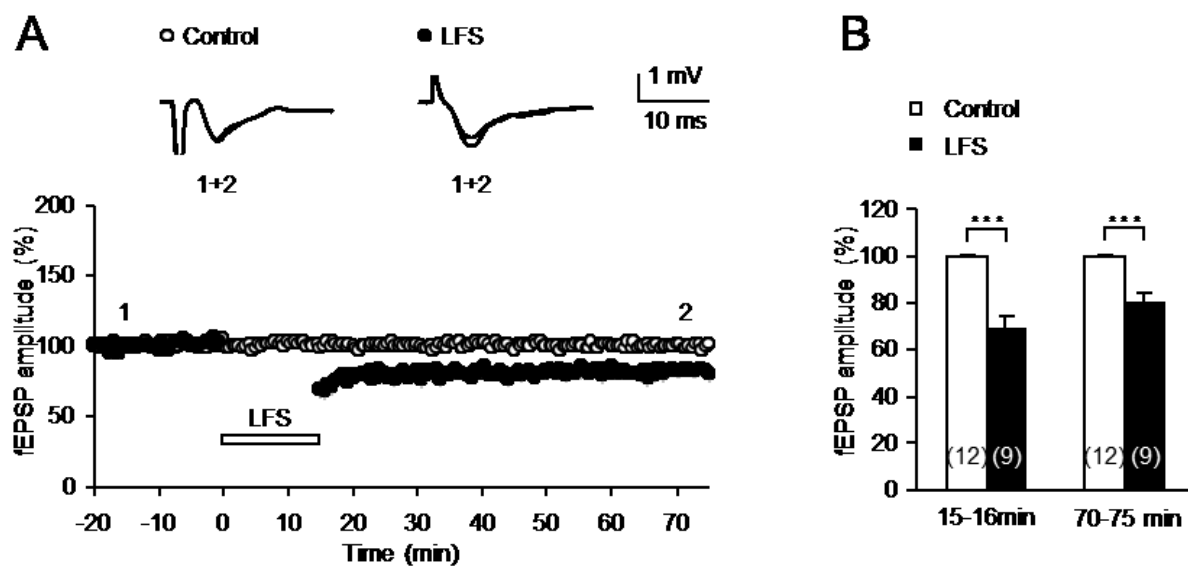
Figure 7: LFS-induced LTD in the medial perforant path in early postnatal rats

(A) The time course of the excitatory postsynaptic field potential (fEPSP) amplitude following stimulation of the medial perforant path (MPP) in early postnatal rats (P9–15) displays LTD (closed symbols) following low-frequency stimulation (LFS, indicated by an open bar). Time-control experiments without LFS (open symbols) confirmed stable recording conditions. Representative fEPSPs were taken at the beginning (indicated by "1") and at the end (indicated by "2") of the experiment. **(B)** The bar graph shows the comparison of the fEPSP levels at time points immediately after application of LFS and end of the experiments in both conditions (control experiments without LFS in open bar and LFS-induced LTD experiments in closed bar). Number of slices is given in parentheses and significant differences are marked by asterisks.

In order to know the effect of 10 µM ZD7288 on LFS-induction of LTD, this compound was bath applied 10 minutes prior to LFS (Figure 8A, closed symbols, n = 7). In these experiments, fEPSP amplitudes both immediately after LFS (STD) and at the end of the experiment (LTD) were more markedly depressed (51 ± 5% and 48 ± 3%, n = 7). However, this enhanced STD and LTD could be biased by the synaptic depression following ZD7288 (Chen, 2004;Chevaleyre and Castillo, 2002). Therefore, interleaved time-control experiments without LFS (Figure 8A, open symbols and Figure 8B, open bar, n = 7) was performed again and indeed obtained a synaptic depression when ZD7288 was bath applied to the slices (80±2% at the end of the experiment; open symbols in Figure 8A and open bar in Figure 8B).
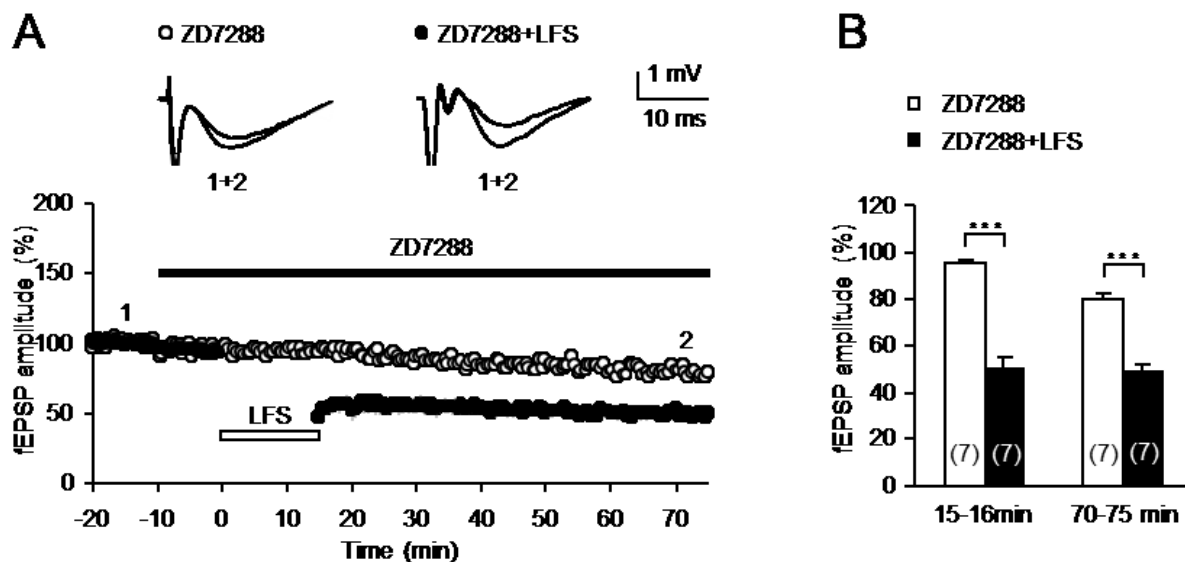
Figure 8: Influence of ZD7288 pre-application on LFS-induced LTD in early postnatal rats

(A) The time course of the fEPSP amplitude following ZD7288 treatment (starting 10 min prior to LFS, indicated by a closed bar) shows an enhanced depression in LFS-treated slices (closed symbols). Non-LFS-treated time-control experiments (open symbols) showed a synaptic depression after ZD7288 application. **(B)** Note the large difference of fEPSP amplitudes at the end of the experiment (ZD7288 treated time control experiments in open bar and ZD7288 treated LFS-induced LTD experiments in closed bar) which was more pronounced than that without ZD7288 application in Figure 7.

In order to directly compare LFS-induced LTD with and without HCN channel inhibition, we normalized LFS-treated slices (closed symbols in Figures 7A and 8A) to non-LFS-treated slices (open symbols in Figures 7A and 8A). This normalization indeed revealed that both STD and LTD were significantly enhanced by ZD7288 pre-application as compared to interleaved time-control experiments (STD with ZD7288: $53 \pm 5\%$, STD control: $69 \pm 6\%$; $P < 0.05$; LTD with ZD7288: $62\pm4\%$, LTD control: $80\pm4\%$, $P < 0.01$; Figures 9A and 9B). These results so far indicate that HCN channel activation during LFS appears to constrain both STD and LTD.
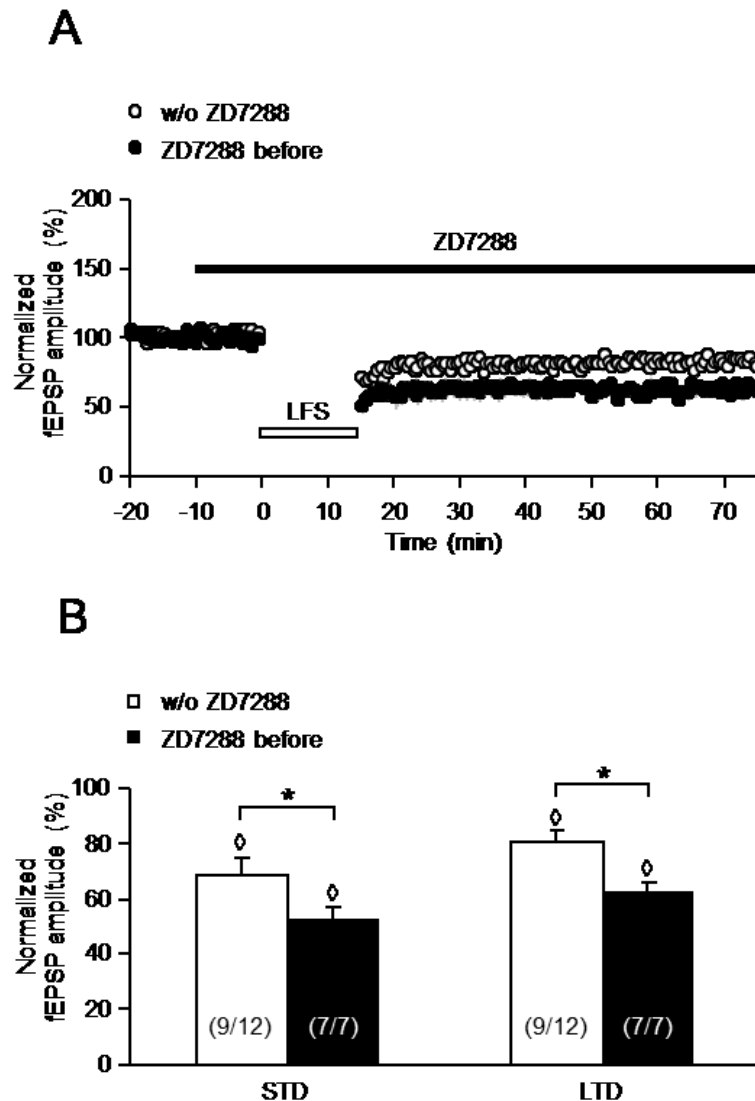
Figure 9: ZD7288 application before LFS enhances LTD in early postnatal rats

(A) Normalized time courses of fEPSP amplitudes in conditions: without ZD7288 (open symbols) and ZD7288 before LFS (closed symbols). **(B)** The bar graph summarizes the STD and LTD levels of two different conditions. Note that both STD and LTD were significantly enhanced by ZD7288 pre-application as compared to interleaved time-control experiments. The number of slices is given in parentheses (number of LFS-treated slices/number of non-LFS-treated slices).

Then a question arose that whether ZD7288 would also exert this effect when applied after LFS has been completed. This is an important control experiment since STD—in this case—is recorded before ZD7288 could actually depress synaptic transmission and thus should not be altered by HCN channel inhibition (Figure 10). In fact, STD was unaltered by ZD7288 treatment after LFS (68 ± 5%, n = 9, gray symbols in Figure 10A and gray bar in Figure 10B). But importantly, fEPSP amplitudes at the end of the experiment were 65 ± 4% in LFS-treated slices and 81 ± 3% in non-LFS-treated control experiments (open symbols in Figure 10A and open bar in Figure 10B).
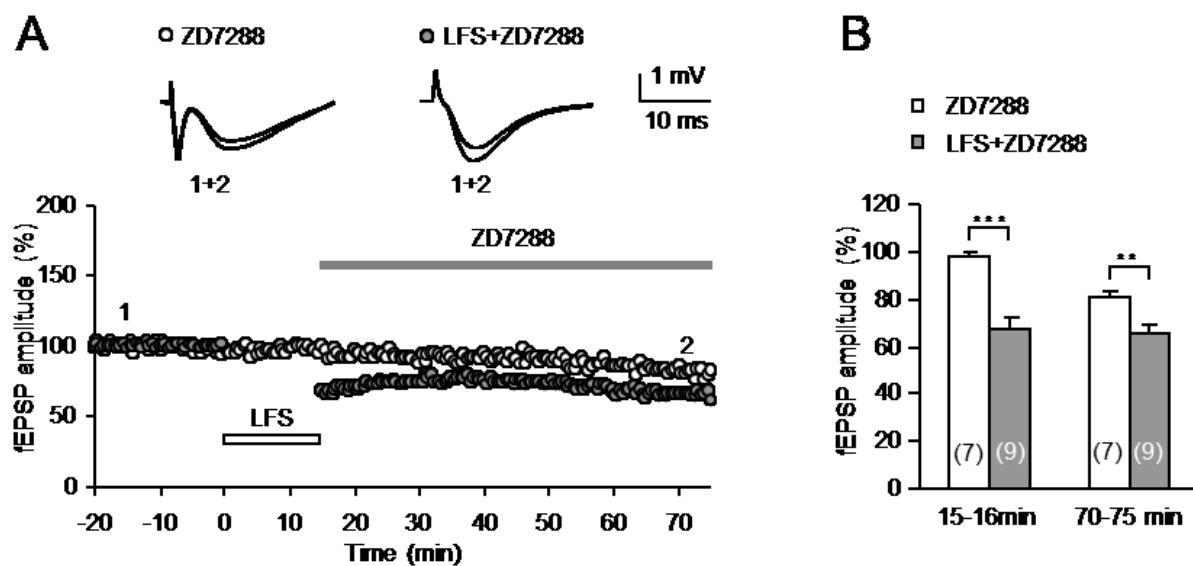
Figure 10: Influence of ZD7288 application after LFS in LFS-induced LTD in early postnatal rats

(A) The time course of the fEPSP amplitude following ZD7288 treatment (starting after LFS, indicated by a gray bar) shows a synaptic depression in both LFS-treated (gray symbols) and non-LFS-treated time-control experiments (open symbols) **(B)** Comparing the fEPSP amplitude between LFS-treated (gray bar) and non-LFS-treated time-control experiments (open bar) reveals a synaptic depression which was similar to that in non-ZD7288 conditions shown in Figure 7.

In order to directly compare the influence of HCN channels on the expression of LFS-induced LTD, we normalized LFS-treated slices to non-LFS-treated slices. Following normalization, both STD and LTD were no longer significantly different from control experiments without ZD7288 application (STD: 68 ± 5%; LTD: 81 ± 5%; gray symbols in Figure 11A and gray bar in Figure 11B). On the one hand, this experiment suggests that the LTD enhancement is a specific ZD7288-mediated effect and not an artifact due to normalization procedure. On the other hand, these data also indicate that HCN channel activation modulate the induction but not the expression of LFS-induced LTD.
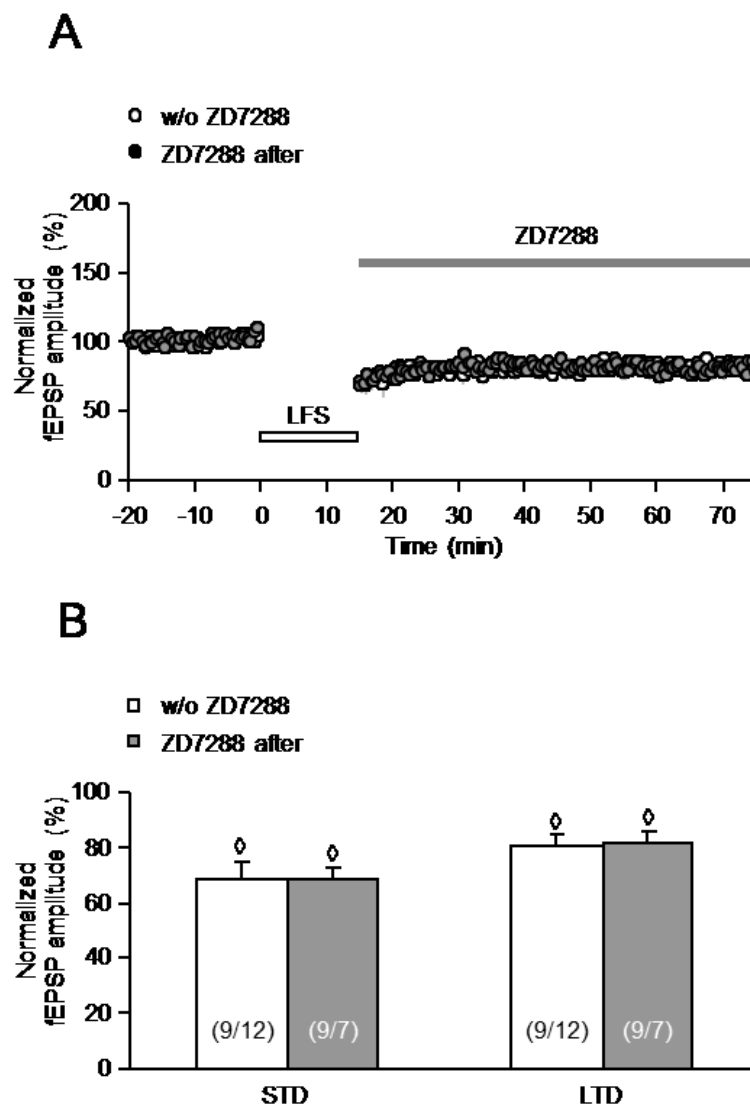
Figure 11: ZD7288 application after LFS has no effect on LFS-induced LTD in early postnatal rats

(A) Normalized time courses of fEPSP amplitudes in conditions: without ZD7288 (open symbols) and ZD7288 after LFS (gray symbols). **(B)** Note that similar levels of LFS-induced STD and LTD were obtained in both slices without ZD7288 and slices with ZD7288 after LFS.

Another important pitfall in recording MPP-evoked fEPSPs is the potential contamination by field potentials following stimulation of the adjacent fiber tract—the lateral perforant path (LPP). The propensity of LTD to be obtained in the middle molecular layer may actually vary with the degree of contamination by LPP stimulation. Therefore, the paired-pulse ratio (PPR) was analyzed in all six experimental groups at the beginning of the experiment, that is, before LFS and/or ZD7288 was applied. As shown in Figure 12, there were no significant differences in the PPR between all groups (on average 76%), thus indicating a negligible contamination by LPP-evoked field potentials.
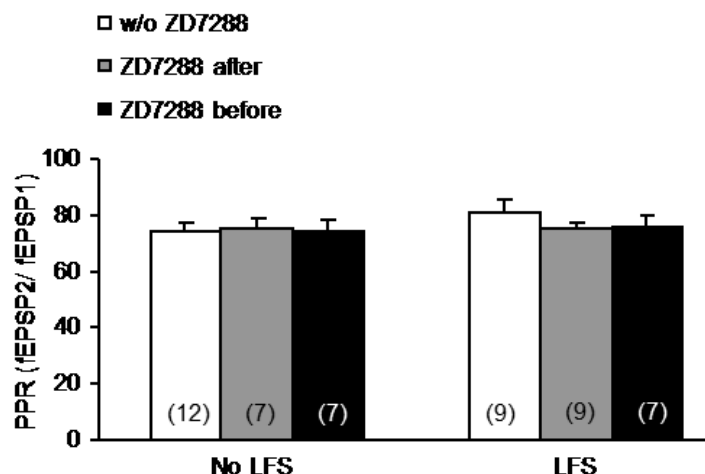
Figure 12: No significant differences in PPR between early postnatal groups

The bar graph summarizes the paired-pulse ratio of all experimental groups recorded at the beginning of each experiment, that is, before ZD7288 and/or LFS were applied to the slices. Note that the PPR was similar in all groups. All data are mean ± SEM.

3.1.2. LFS-induced LTD in adult rats is not affected by ZD7288

The results presented so far indicated a constraining effect of HCN channels on LFS-induced LTD in early postnatal MPP-dentate gyrus synapses. Then a question was asked that whether this LTD enhancement following ZD7288 treatment was due to an inhibition of presynaptic HCN channels that are abundant in immature MPP, but disappear with aging (Bender et al., 2007). Therefore these experiments were repeated with adult rats (P30-60).

In slices taken from these animals, LFS applied to the MPP caused a short-term depression to 82 ± 2% of the baseline fEPSP amplitude (Figure 13A in closed symbols and Figure 13B in closed bar, n = 6) and resulted in stable LTD of 81 ± 3% of baseline at 60 minutes after LFS. Interleaved time-control experiments without LFS demonstrated that our recording conditions were again stable for at least 90 minutes (100 ± 2% at the end of the experiment; open symbols in Figure 13A and open bar in Figure 13B, n = 8).
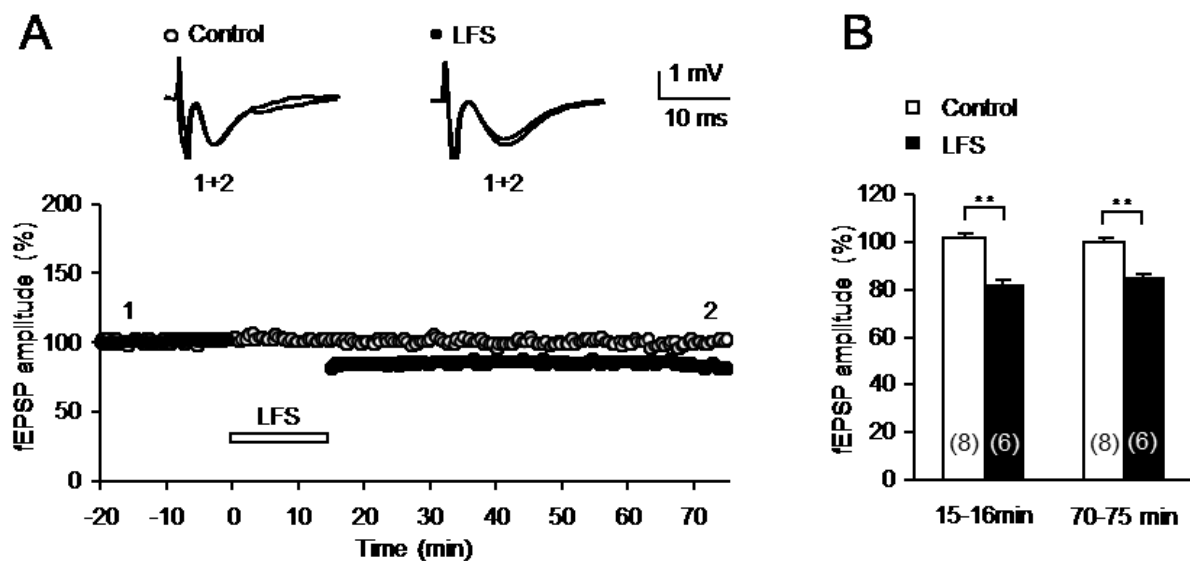
Figure 13: LFS-induced LTD in the medial perforant path in adult rats

(A) The time course of the fEPSP amplitude following LFS in adult rats (P30–60) shows LTD (closed symbols) as compared to time-control experiments without LFS (open symbols). Representative fEPSPs were taken at the beginning (indicated by "1") and at the end (indicated by "2") of the experiment. **(B)** The bar graph displays the comparison of the fEPSP levels at time points immediately after application of LFS and end of the experiments in both conditions (control experiments without LFS in open bar and LFS-induced LTD experiments in closed bar). Number of slices is given in parentheses and significant differences are marked by asterisks.

As in early postnatal rats, The effect of 10µM ZD7288 on LFS-induced LTD was studied and thus this compound was applied 10 minutes prior to LFS (Figure 14A, closed symbols, n = 9). Under HCN channel blocking conditions, both STD and LTD appeared to be more depressed as compared to slices without ZD7288 treatment (63 ± 4% and 65 ± 4%, closed bar in Figure 14B, n = 9). However, this enhanced STD and LTD could again be biased by ZD7288-mediated synaptic depression, and interleaved time-control experiments without LFS (Figure 14A, open symbols, n = 6) indeed revealed a significant synaptic depression to 77 ± 4% at the end of the experiment (open bar in Figure 14B).
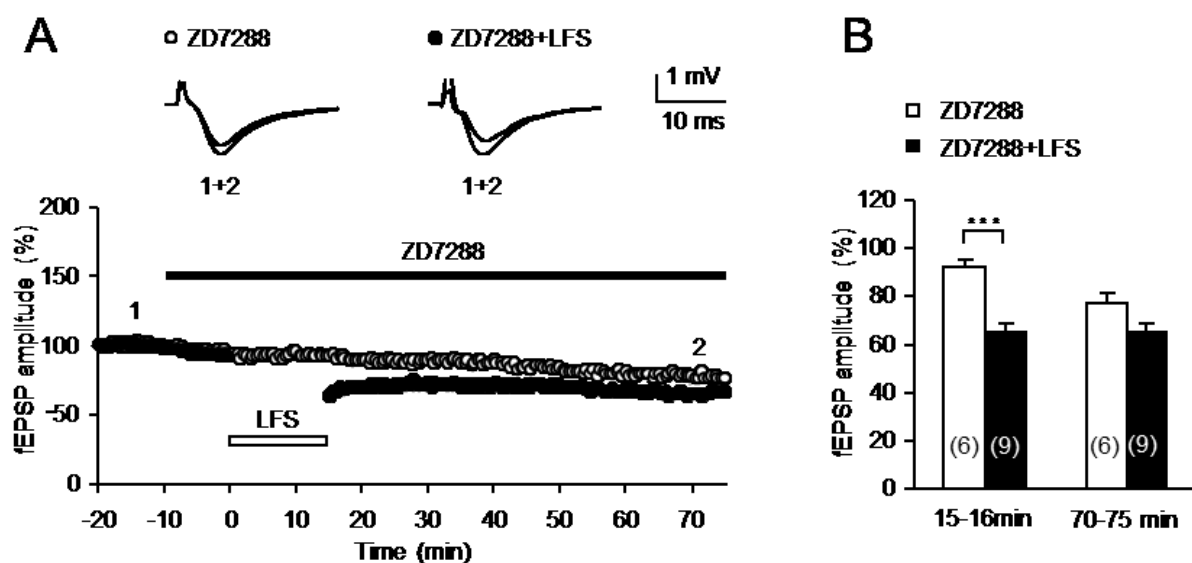
Figure 14: Influence of ZD7288 pre-application in LFS-induced LTD in adult rats

(A) The time course of the fEPSP amplitude following ZD7288 treatment (starting 10 min prior to LFS, indicated by a closed bar) shows a synaptic depression in both LFS-treated (closed symbols) and non-LFS-treated time-control experiments (open symbols). **(B)** Comparing the fEPSP amplitude between LFS-treated (closed bar) and non-LFS-treated time-control experiments (open bar) reveals a synaptic depression which was similar to that in non-ZD7288 conditions shown in Figure 13.

Since ZD7288 itself mediates synaptic depression, it was again necessary to normalize LFS-treated slices (closed symbols in Figures 13A and 14A) to non-LFS-treated slices (open symbols in Figures 13A and 14A). In contrast to slices from early postnatal rats, the normalized values for both STD and LTD were no longer significantly different between ZD7288-treated and ZD7288-untreated conditions (STD with ZD7288: 70 ± 4%, STD control: 81 ± 5%; LTD with ZD7288: 85 ± 5%, LTD control: 85 ± 6%, Figures 15A and 15B). Thus, HCN channel activation failed to have a significant effect on STD and LTD in adult rats.
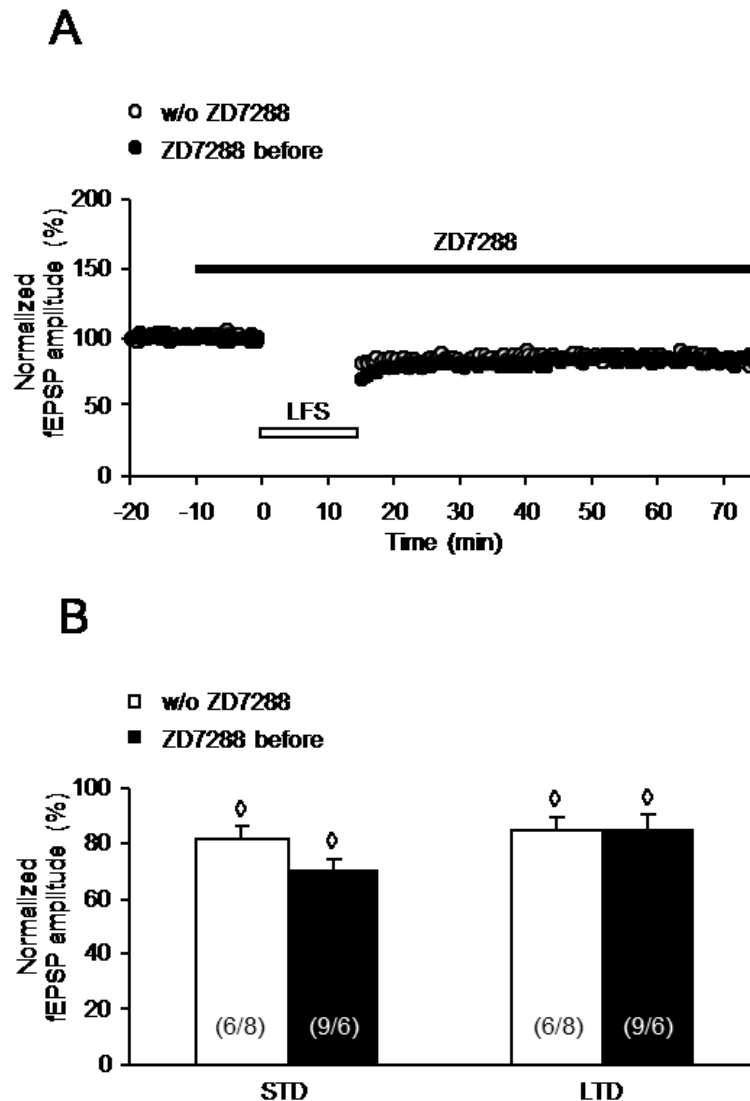
Figure 15: ZD7288 failed to have effect on LFS-induced LTD in adult rats

(A) Normalized time courses of fEPSP amplitudes in both conditions: without ZD7288 (open symbols) and ZD7288 before LFS (closed symbols). Note that similar levels of LFS-induced STD and LTD were obtained in both slices without ZD7288 and slices with ZD7288 before LFS. **(B)** The bar graph summarizes the STD and LTD levels in both ZD7288 (open bar) and non-ZD7288 conditions (closed bar). The number of slices is given in parentheses (number of LFS-treated slices/number of non-LFS-treated slices).

There were no significant differences in the PPR between all groups again (on average 80%, Figure 16) and a contamination by LPP-evoked field potentials is therefore unlikely.
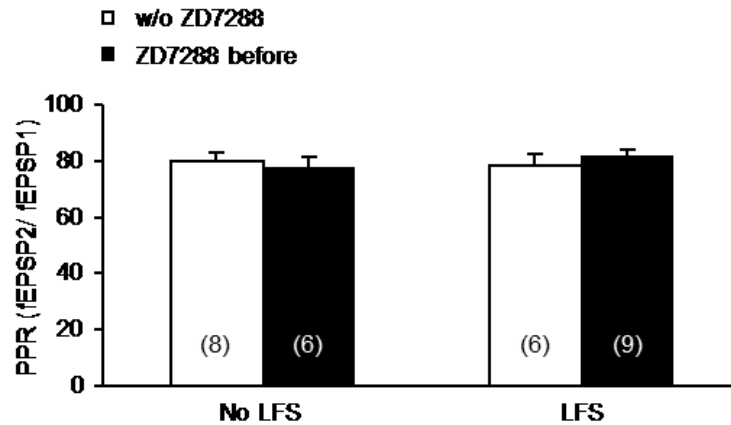
Figure 16: No significant differences in PPR between adult groups

The bar graph summarizes the paired-pulse ratio of all experimental groups recorded at the beginning of each experiment, that is, before ZD7288 and/or LFS were applied to the slices. Note that the PPR was similar in all groups. All data are mean ± SEM.

3.1.3. LFS-induced LTD at MPP is NMDA receptor dependent

These results may suggest that HCN channel-mediated suppression of LFS-induced LTD is downregulated during developmental maturation. However, one could argue that LFS-induced LTD in different ages may involve different induction mechanisms. Therefore a question was asked that whether NMDA receptors are required for LTD induction in both age groups and our experiments were repeated in the presence of the NMDA receptor antagonist D-AP5 (50µM). In fact, LTD was abolished under these conditions in both adult (95 ± 7%, n = 5) and early postnatal rats (95 ± 3%, n = 8; Figures 16A and 16B; both age groups P < 0.05 versus untreated slices). Hence, differential NMDA receptor dependence of LTD induction cannot explain the differences in immature and adult tissues.
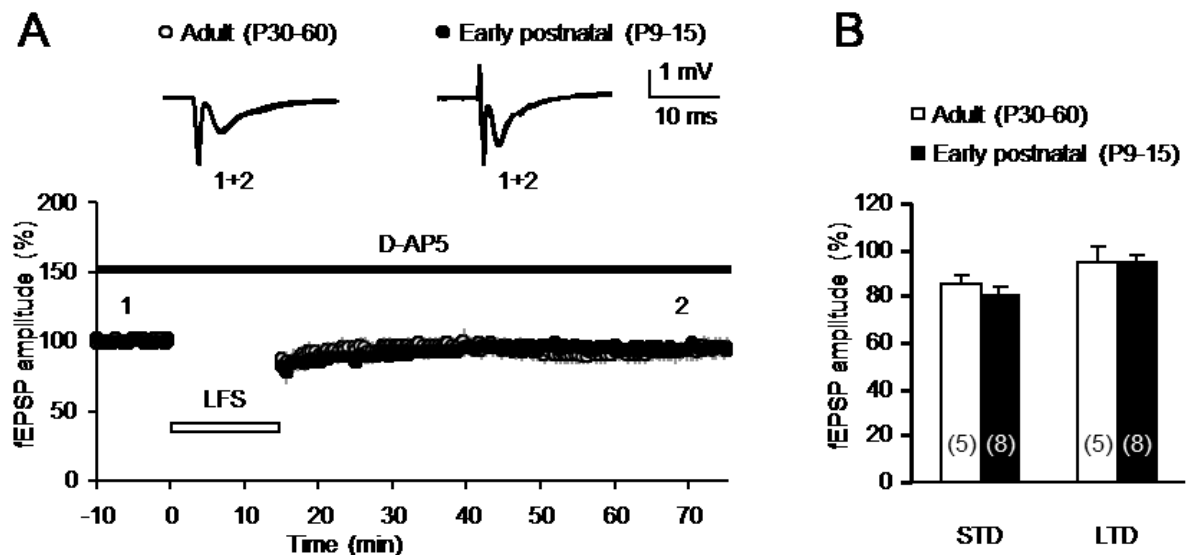
Figure 17: LFS-induced LTD in MPP is NMDA receptor dependent in both adult and early postnatal rats

(A) The time course of the fEPSP amplitude following LFS in adult (P30–60, open symbols) and early postnatal rats (P9–15, closed symbols) shows no LTD in the presence of the NMDA receptor blocker D-AP5 (50 µM, indicated by a black bar). Representative fEPSPs were taken at the beginning (indicated by "1") and at the end (indicated by "2") of the experiment. (B) The bar graph summarizes the STD and LTD levels in both adult (open bars) and early postnatal rats (closed bars) in the presence of D-AP5.

3.1.4. ZD7288 increase PPR in early postnatal, but not in adult rats

Since immature MPP axon terminals express presynaptic HCN channels that have been demonstrated to be downregulated upon maturation (Bender et al., 2007). Thus, a question arose, whether ZD7288 might alter the paired-pulse ratio (PPR) in slices from early postnatal and adult rats (Figure 18). Initial experiments revealed that bath application of ZD7288 occasionally led to an exacerbation of disinhibitory network activity, probably due to gabazine which was present in all our solutions. Therefore, we first recorded a baseline with paired-pulse stimulation, then incubated the slices with ZD7288 (10µM) while switching off the stimulation for 15min, and finally delivered paired-pulse stimulation again for another 20min (Figures 18A and 18B). As shown previously (Figures 8 and 14), ZD7288 generally depressed MPP-evoked fEPSPs. However, in slices from immature rats, the field potential evoked by the first stimulus (fEPSP1, gray boxes in Figure 18A) appeared to be more affected by this compound than the second response (fEPSP2, gray diamonds in Figure 18A). As a consequence, ZD7288 caused a significant increase of the normalized paired-pulse ratio (117 ± 4%, n = 8, gray symbols/bars in Figures 18C and 18D). In adult rats, however, ZD7288 depressed the first and second fEPSP to the same degree resulting in no significant change of the PPR (98 ± 2%, n = 11, open symbols/bars in Figures 18C and 18D). These findings indicate that HCN channel blockade causes a reduction of fEPSP amplitudes in both immature and adult tissues. But, in addition, it leads to an increase of the paired-pulse ratio only in immature synapses suggesting that presynaptic HCN channels facilitate glutamate release.
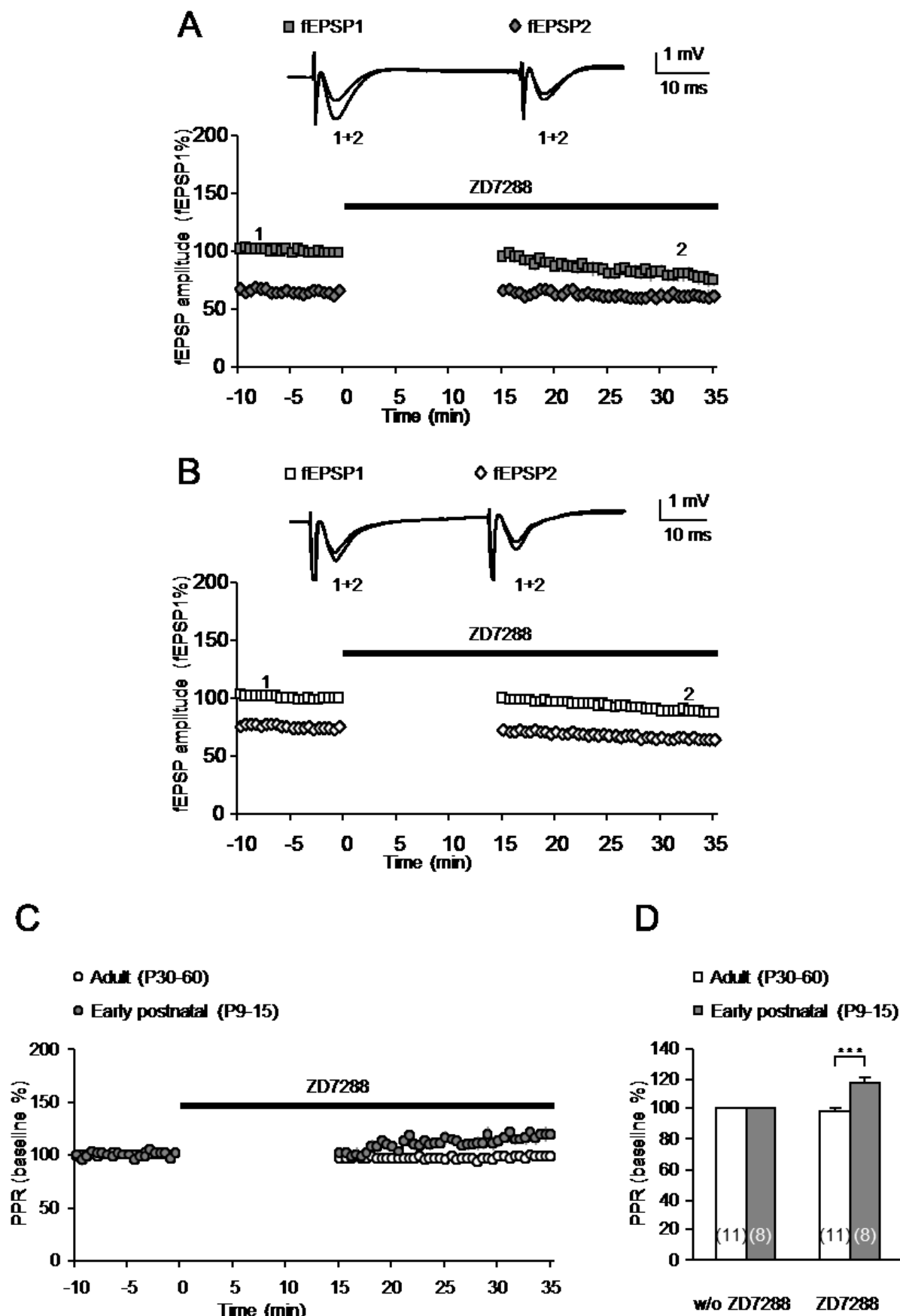
Figure 18

Figure 18: ZD7288 enhances the paired-pulse ratio in early postnatal rats, but not in adults

(A) The time course of the fEPSP amplitudes (normalized to the fEPSP1 baseline) following paired-pulse stimulation (interpulse interval 40 ms) delivered to the MPP in early postnatal rats (P9–15) shows that ZD7288 (indicated by a black bar) depressed the first response (fEPSP1, gray boxes) more markedly than the second response (fEPSP2, gray diamonds). Representative fEPSPs were taken at the beginning (indicated by "1") and at the end (indicated by "2") of the experiment. **(B)** The time course of the fEPSP amplitudes (normalized to the fEPSP1 baseline) following paired-pulse stimulation (interpulse interval 40 ms) delivered to the MPP in adult rats (P30–60) shows that ZD7288 (black bar) depressed the first (fEPSP1, open boxes) and the second response (fEPSP2, open diamonds) to the same degree. Representative fEPSPs were taken at the beginning (indicated by "1") and at the end (indicated by "2") of the experiment. **(C)** Time courses of the PPR (normalized to baseline PPR) in both age groups: adult (open symbols) and early postnatal rats (gray symbols). Note that ZD7288 increased PPR only in early postnatal animals. **(D)** The bar graph summarizes the normalized paired-pulse ratio of both age groups recorded before and after ZD7288 treatment. ZD7288 significantly increased the PPR in early postnatal, but not in adult, animals. All data are mean ± SEM.

3.2. LFS-induced LTD in early postnatal, but not in adult rats, is enhanced by NOS inhibitor L-NAME

This finding so far indicate that LFS-induced LTD is NMDA receptor dependent and— in the case of early postnatal synapses—is compromised by HCN channel activation. If indeed presynaptic HCN channels might be responsible for this modulation in immature tissue, a retrograde signaling pathway has to be postulated to transfer the information of postsynaptic NMDA receptor activation to presynaptic HCN channels. One major retrograde messenger is nitric oxide (NO) produced by postsynaptic NO synthase (NOS) which travels through the synaptic cleft to activate presynaptic guanylate cyclases (Neitz et al., 2011;Stanton et al., 2003).

This hypothesis was tested by repeating these experiments in the presence of the NOS blocker L-NAME (100µM), and this compound was bath applied 10 min prior to LFS. In these experiments, fEPSP amplitudes both STD and LTD were more markedly depressed (closed symbols in Figure 19A and closed bar in Figure 19B; STD: 62 ± 5% and LTD: 66 ± 6%, n = 7) in early postnatal rats. Interleaved time-control experiments without LFS display that L-NAME itself had no effect on MPP-evoked fEPSPs (open symbols in Figure 19A, and open bar in Figure 19B, 100 ± 6%, n = 7).
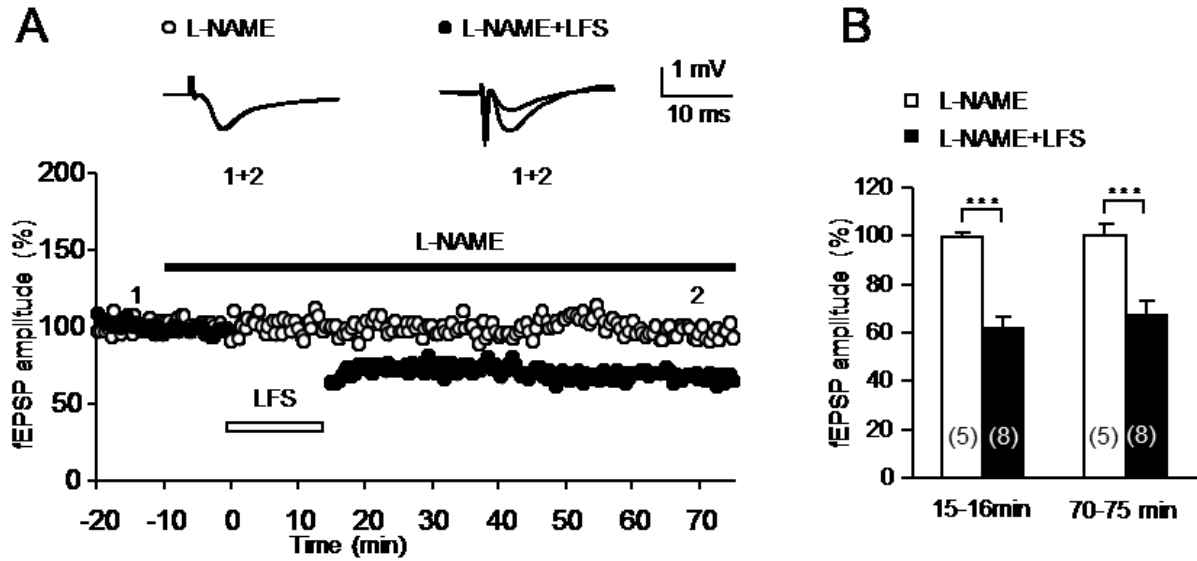
Figure 19: Influence of L-NAME on LFS-induced LTD in early postnatal rats

(A) The time course of the fEPSP amplitude following LFS in early postnatal rats (P9–15) shows robust LTD (closed symbols) as compared to time-control experiments without LFS (open symbols). L-NAME (100 µM) was applied 10 min prior to LFS (indicated by a lack bar). Representative fEPSPs were taken at the beginning (indicated by "1") and at the end (indicated by "2") of the experiment. **(B)** Note the large difference of fEPSP amplitudes at the end of the experiment (L-NAME treated time control experiments in open bar and L-NAME treated LFS-induced LTD experiments in closed bar) which was more pronounced than that in control conditions without L-NAME application (Figure 7). Number of slices is given in parentheses and significant differences are marked by asterisks.

The same procedure as in early postnatal rats, 100µM L-NAME was bath applied 10 min prior to LFS to slices from adult animals. In these experiments, fEPSP amplitudes at the end of the experiment were 84 ± 3% in LFS-treated slices (closed symbols in Figure 20A and closed bar in Figure 20B) and 101 ± 2% in non-LFS-treated control experiments showing L-NAME itself had no effect on MPP-evoked fEPSPs (open symbols in Figure 20A and open bar in Figure 20B).
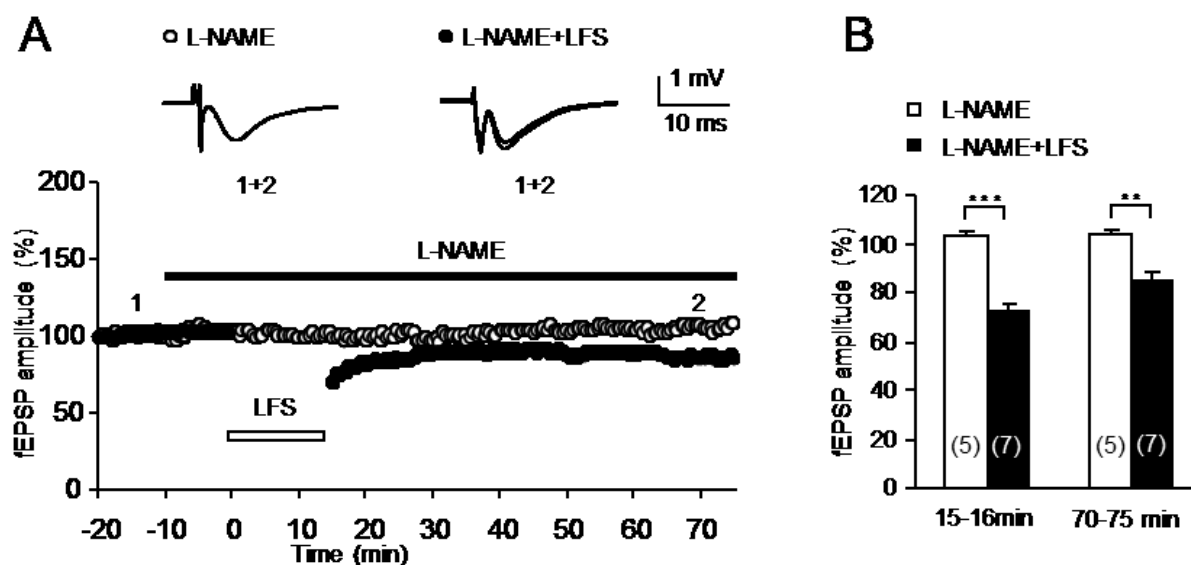
Figure 20: Influence of L-NAME on LFS-induced LTD in adult rats

(A) The time course of the fEPSP amplitude following LFS in adult rats (P30–60) also shows LTD (closed symbols) as compared to time-control experiments without LFS (open symbols). L-NAME (100 µM) was applied 10 min prior to LFS (indicated by a lack bar). Note that less LTD was obtained when compared to early postnatal animals (Figure 19). Representative fEPSPs were taken at the beginning (indicated by "1") and at the end (indicated by "2") of the experiment. **(B)** Note that the fEPSP amplitude at the end of the experiment (LFS-treated in closed bar and non-LFS-treated time-control experiments in open bar) was similar to that in non-L-NAME conditions shown in Figure 13.

L-NAME itself had no effect on MPP-evoked fEPSPs in both age groups (early postnatal: open symbols in Figure 19A; adult: open symbols in Figure 20A). Normalization to non-LFS-treated slices revealed that L-NAME significantly enhanced LTD in early postnatal tissue (66 ± 6%, n = 7, Figure 21A in closed bar), when compared to control conditions (80 ± 4%, n = 9; P < 0.05, Figure 21A in open bar). This modulatory role of L-NAME was lost in adult tissue (with L-NAME: 81 ± 3%, n = 7; without L-NAME: 85 ± 6%, n = 6, Figure 21A). The PPR analysis of all L-NAME-treated slices (on average 78%) did not detect any significant differences, thus arguing against LPP contamination (Figure 21B).
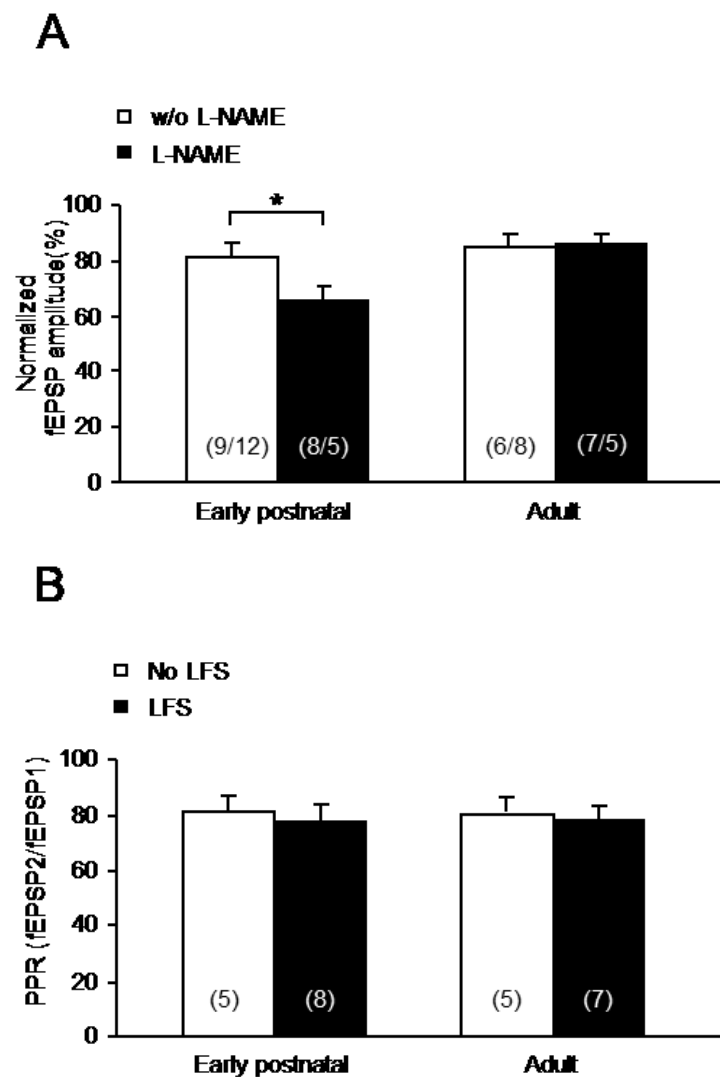
Figure 21: L-NAME enhances LFS-induced LTD in early postnatal, but not adult, rats

(A) The bar graph summarizes the LTD levels for slices treated with L-NAME (closed bars). For the sake of clarity, data from Figures 9(B) and 15(B) is also shown in order to illustrate non-L-NAME conditions (open bars). The number of slices is given in parentheses (number of LFS-treated slices/number of non-LFS-treated slices). **(B)** The bar graph summarizes the paired-pulse ratio of all experimental groups recorded at the beginning of each experiment, that is, before L-NAME and/or LFS were applied to the slices. Note that the PPR was similar in all groups. All data are mean ± SEM.

These results obtained with L-NAME are reminiscent of the effect of HCN channel inhibition on LFS-induced LTD and suggest that retrograde signaling with NO might play a major role in the linkage between postsynaptic NMDA receptor activation and presynaptic HCN channel function.

3.3. Influence of ZD7288 and L-NAME coapplication on LFS-induced LTD at MPP–granular cell synapses

3.3.1. LFS-induced LTD is enhanced by co-application of ZD7288 and L-NAME in early postnatal rats

These findings so far indicated that both HCN channel blocker ZD7288 and NOS inhibitor L-NAME enhanced LFS-induced LTD in early postnatal synapses. Because HCN channels are known to be also modulated by guanosine cyclic monophosphate (cGMP), a cellular regulatory agent and which has been described as a second messenger, we hypothesized that the effects of these two blockers are mediated by the same pathways. Generation of cGMP in the presynapse via NO retrograde signaling pathway might affect HCN channel activities in the MPP terminals.

In order to clarify this, we conducted additional experiments by bath-application of ACSF containing both ZD7288 (10 µM) and L-NAME (100µM). Similar to our previous data obtained by application of either ZD7288 or L-NAME, co-application of these compound 10 minutes prior to LFS caused marked reduction of fEPSPs inducing significant STD and LTD (STD: $48 \pm 3\%$, LTD: $52 \pm 5\%$, n =8; Figure 22C and 22D, closed symbols) as compared to the control conditions without presence of any blockers (STD: $68 \pm 7\%$ and LTD: $83 \pm 2\%$, n =4; Figure 22A and 22B, closed symbols). However, the enhancement of STD and LTD could again be biased by ZD7288-mediated synaptic depression (Figure 22C, closed symbols), because interleaved time-control experiments without LFS (Figure 22C, open symbols) revealed a significant synaptic depression to $85 \pm 2\%$ at the end of the experiment (open bar in Figure 22D, n = 7). Time-control experiments without LFS (open symbols in Figure 22A and open bar in Figure 22B; n = 8) confirmed stable recording conditions.
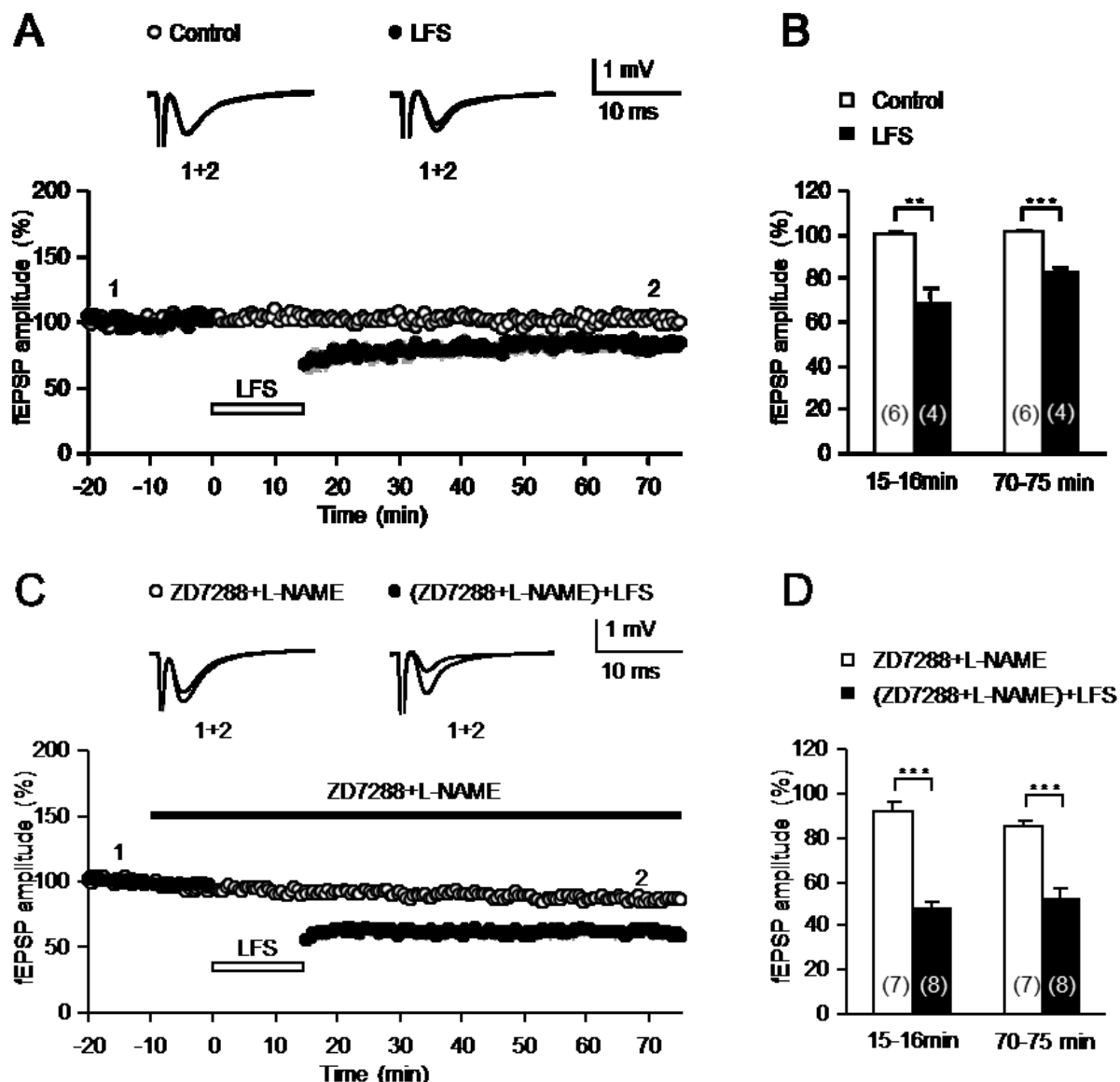
Figure 22: Influence of ZD7288 and L-NAME on LFS-induced LTD in early postnatal rats

(A) The time course of fEPSP amplitude following LFS on MPP in early postnatal rats (P9–15) displays LTD (closed symbols) as compare to time-control experiments without LFS (open symbols). Representative fEPSPs were taken at the beginning (indicated by "1") and at the end (indicated by "2") of the experiment. **(B)** The bar graph shows the comparison of the fEPSP levels at time points immediately after application of LFS and end of the experiments in both conditions (control experiments without LFS in open bar and LFS-induced LTD experiments in closed bar). Number of slices is given in parentheses and significant differences are marked by asterisks. **(C)** The time course of the fEPSP amplitude following ZD7288+L-NAME treatment (starting 10 min prior to LFS, indicated by a closed bar) shows an enhanced depression in LFS-treated slices (closed symbols). Non-LFS-treated time-control experiments (open symbols) showed a synaptic depression after co-application of ZD7288+L-NAME. **(D)** Note the large difference of fEPSP amplitudes at the end of the experiment (ZD7288+L-NAME treated time control experiments in open bar and ZD7288+L-NAME treated LFS-induced LTD experiments in closed bar) which was more pronounced than that without ZD7288+L-NAME in (A) and (B).

In order to get pure results, we normalized LFS-treated slices (closed symbols in Figures 22A and 22C) to non-LFS-treated slices (open symbols in Figures 22A and 22C). This normalization indeed revealed that LTD was significantly enhanced by co-application of ZD7288 and L-NAME (STD: 53 ± 3%; LTD: 61±6%; n=8/7; Figures 23A and 23B) as compared to interleaved time-control experiments (STD: 66 ± 7%; LTD: 82±2%, 4/6; P < 0.05; Figures 23A and 23B). These results indicate that LFS-induced LTD could also be enhanced by simultaneous blockade of both HCN channels and NOS. Finally, as shown in Figure 23C, there were no significant differences in the PPR between all groups (on average 70%), thus indicating a negligible contamination by LPP-evoked field potentials.

A

B

C
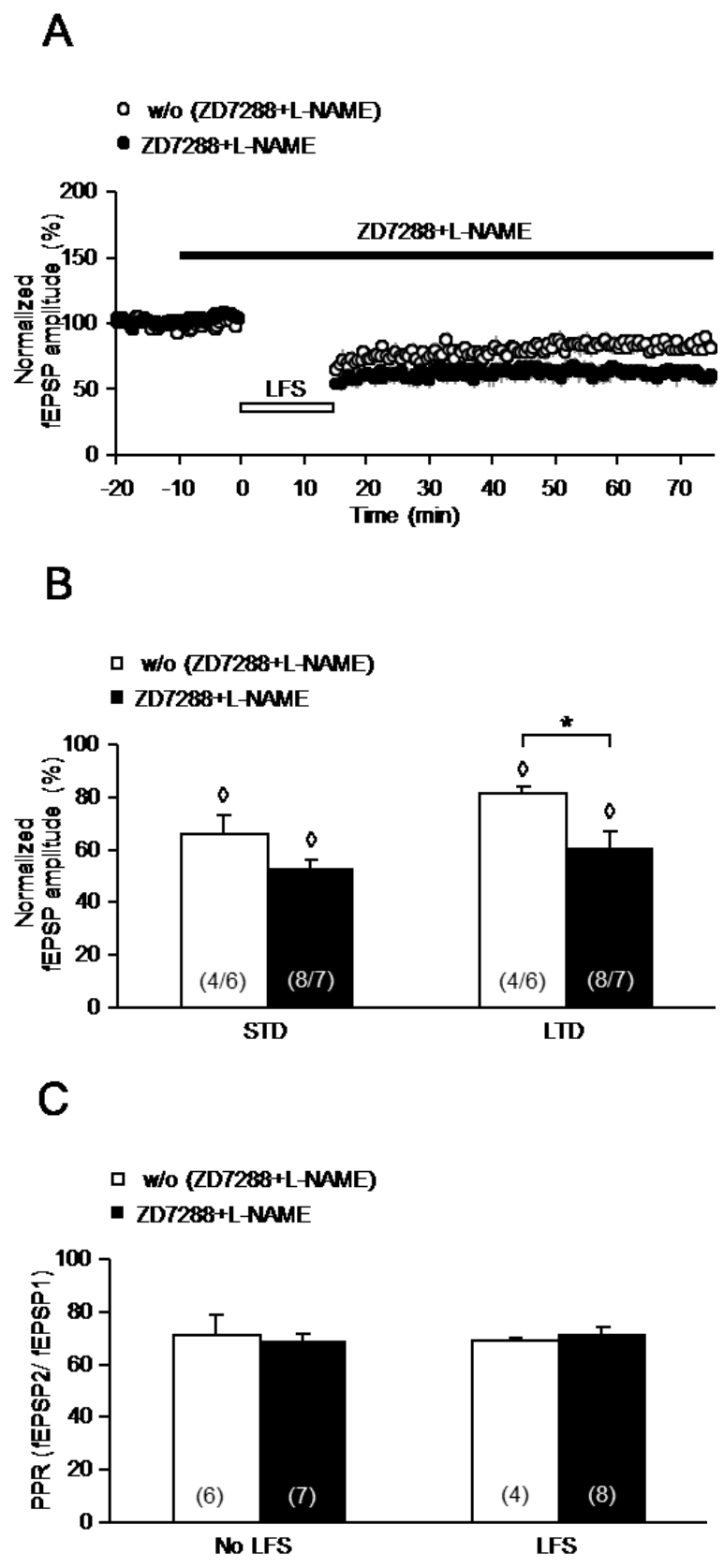
Figure 23

Figure 23: Co-application of ZD7288 and L-NAME enhances LTD in early postnatal rats

(A) Normalized time courses of fEPSP amplitudes in conditions: without (ZD7288+L-NAME) treated (open symbols) and (ZD7288+L-NAME) treated (closed symbols). **(B)** The bar graph summarizes the STD and LTD levels of two different conditions. Note that both STD and LTD were significantly enhanced by ZD7288 and L-NAME co-application as compared to interleaved time-control experiments. The number of slices is given in parentheses (number of LFS-treated slices/number of non-LFS-treated slices). **(C)** The bar graph summarizes the paired-pulse ratio of all experimental groups recorded at the beginning of each experiment, that is, before ZD7288+L-NAME and/or LFS were applied to the slices. Note that the PPR was similar in all groups. All data are mean ± SEM.

3.3.2. LFS-induced LTD in adult rats is not affected by co-application of ZD7288 and L-NAME

As in early postnatal rats, the effect of 10µM ZD7288 and 100µM L-NAME on LFS-induced LTD was studied in adult rats. Thus, as shown in Figure 24C, ACSF containing these compounds were bath-applied 10 minutes prior to LFS. Under this conditions, both STD and LTD appeared to be more depressed (78 ± 3% and 68 ± 4%, n =8, closed symbols in Figure 24C and closed bar in Figure 24D) as compared to slices without any drug treatment (72 ± 2% and 85 ± 3%, n=9, closed symbols in Figure 24A and closed bar in Figure 24B). However, this enhanced STD and LTD could again be biased by ZD7288-mediated synaptic depression, and interleaved time-control experiments without LFS (Figure 24C, open symbols, n = 9) indeed revealed a significant synaptic depression to 80 ± 5% at the end of the experiment (open bar in Figure 24D). Time-control experiments without LFS (open symbols in Figure 24A and open bar in Figure 24B) confirmed stable recording conditions.
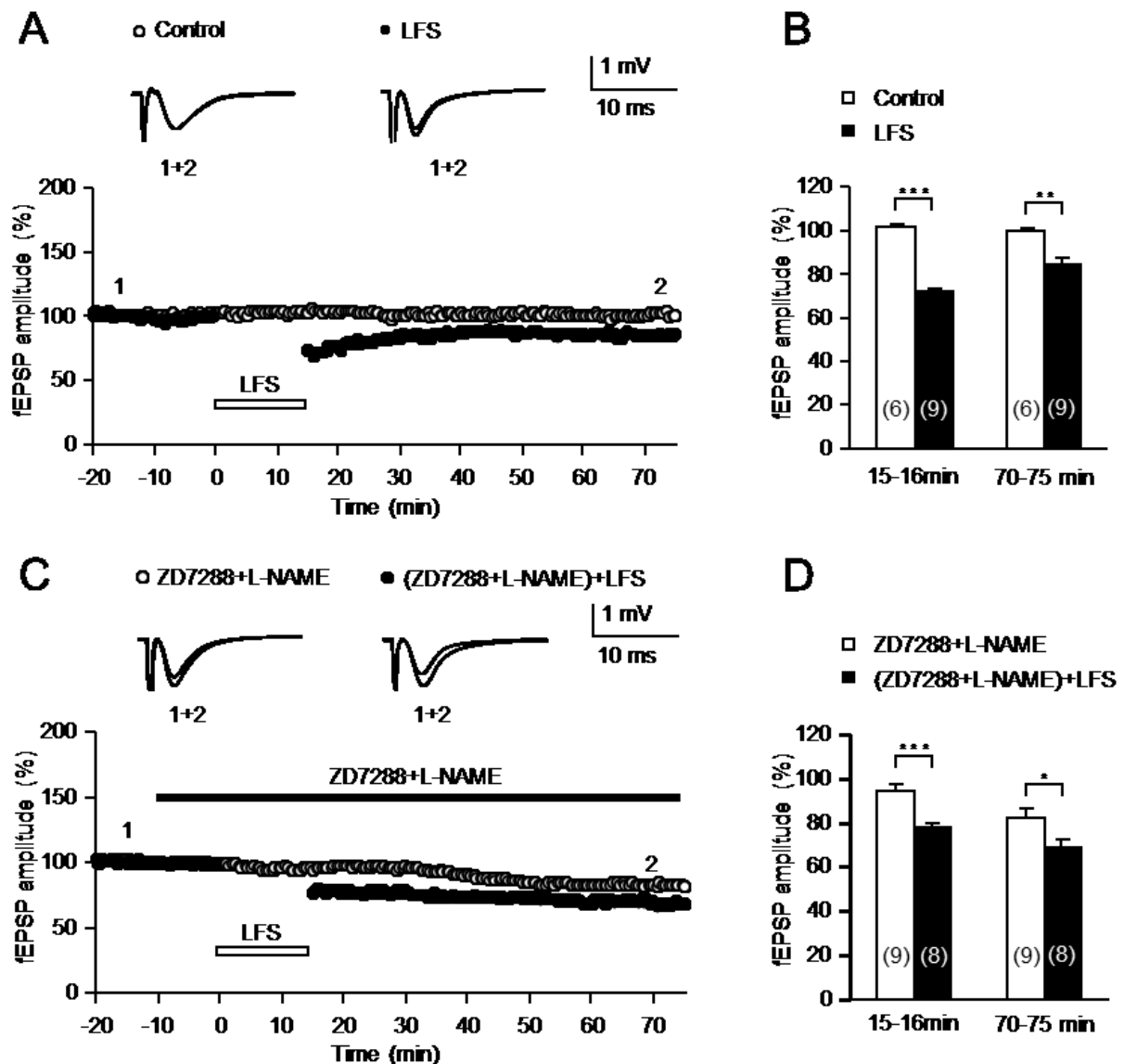
Figure 24: Influence of ZD7288 and L-NAME on LFS-induced LTD in adult rats

(A) The time course of fEPSP amplitude following LFS on in adult rats (P30–60) shows LTD (closed symbols) as compared to time-control experiments without LFS (open symbols). Representative fEPSPs were taken at the beginning (indicated by "1") and at the end (indicated by "2") of the experiment. **(B)** The bar graph displays the comparison of the fEPSP levels at time points immediately after application of LFS and end of the experiments in both conditions (control experiments without LFS in open bar and LFS-induced LTD experiments in closed bar). Number of slices is given in parentheses and significant differences are marked by asterisks. **(C)** The time course of the fEPSP amplitude following ZD7288+L-NAME treatment (starting 10 min prior to LFS, indicated by a closed bar) shows a synaptic depression in both LFS-treated (closed symbols) and non-LFS-treated time-control experiments (open symbols). **(D)** Comparing the fEPSP amplitude between LFS-treated (closed bar) and non-LFS-treated time-control experiments (open bar) reveals a synaptic depression which was similar to that in non-ZD7288+L-NAME conditions shown in (A) and (B).

Since ZD7288 itself mediated synaptic depression, it was again necessary to normalize LFS-treated slices (closed symbols in Figures 24A and 24C) to non-LFS-treated slices (open symbols in Figures 24A and 24C). In contrast to slices from early postnatal rats, the normalized values for both STD and LTD were no longer significantly different between ZD7288+L-NAME treated (STD: 81 ± 3%; LTD: 86 ± 5%; n= 8/10) and ZD7288+L-NAME untreated conditions (STD: 70 ± 2%; LTD: 85 ± 3%, n= 9/6; Figures 25A and 25B). Thus, the modulatory role of ZD7288+L-NAME was lost in adult rats. There were no significant differences in the PPR between all groups again (on average 77%, Figure 25C) and a contamination by LPP-evoked field potentials is therefore unlikely.

A

B

C
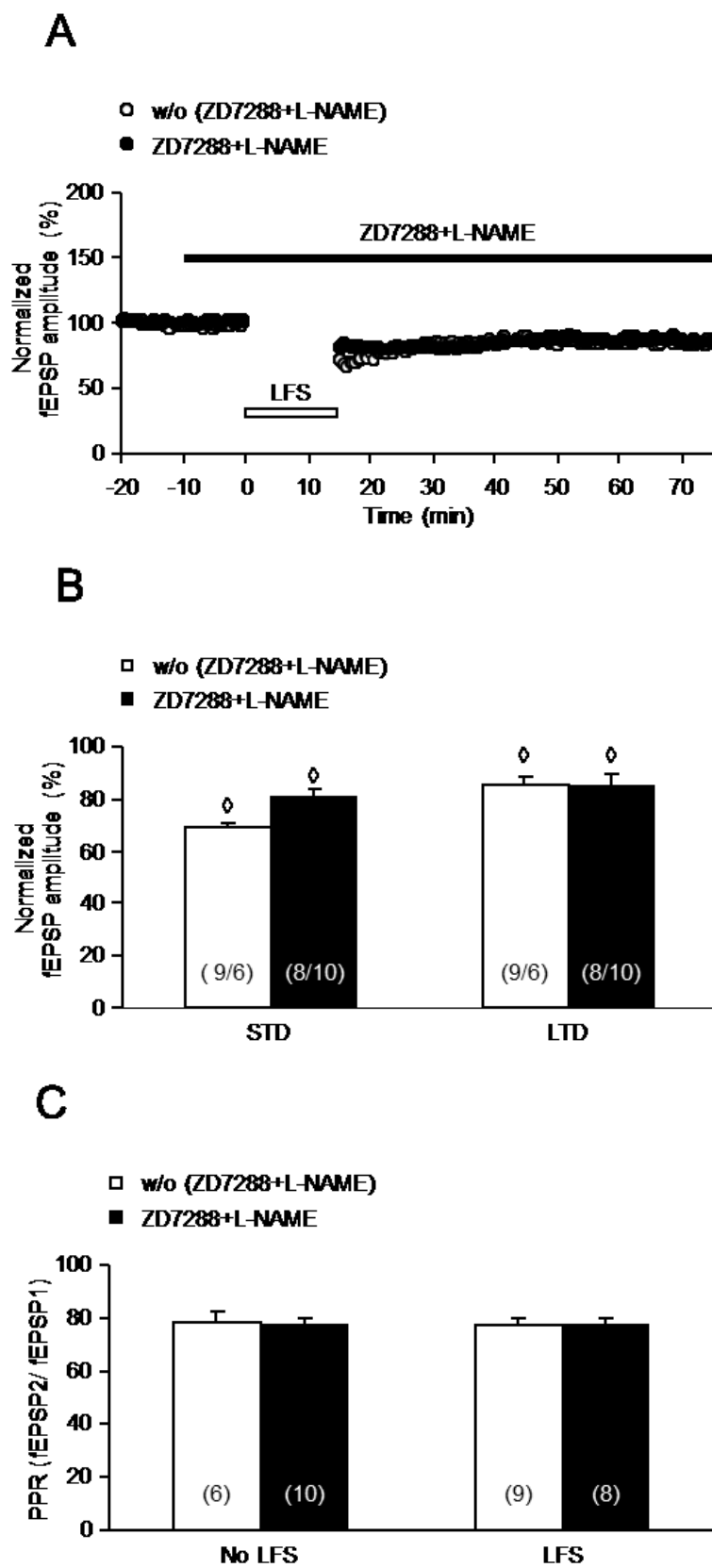
Figure 25

Figure 25: Co-application of ZD7288 and L-NAME failed to have effect on LFS-induced LTD in adult rats

(A) Normalized time courses of fEPSP amplitudes in conditions: without ZD7288+L-NAME treated (open symbols) and with ZD7288+L-NAME treated (closed symbols). Note that similar levels of LFS-induced STD and LTD were obtained in both slices without ZD7288+L-NAME and slices with ZD7288+L-NAME. **(B)** Bar graphs summarize the STD and LTD levels of two different conditions. The number of slices is given in parentheses (number of LFS-treated slices/number of non-LFS-treated slices). **(C)** Bar graphs summarize the paired-pulse ratio (PPR) of all experimental groups recorded at the beginning of each experiment, that is, before ZD7288+L-NAME and/or LFS were applied to the slices. Note that the PPR was similar in all groups. All data are mean ± SEM.

3.4. Summary of LTD results

For the sake of clarity, data already shown in Figures 9B, 11B, 15B, 21A, 23B and 25B are recapitulated in Figure 26 to demonstrate normalized LTD levels in different experimental conditions. As you may notice, in early postnatal rats, fEPSP amplitudes were markedly lower in conditions when slices were perfused with ACSF containing ZD7288 (before LSF), L-NAME and ZD7288+L-NAME, indicating more LTD induction in these groups. Statistical analyses show LTD enhancement observed in these groups are all significantly different from control group, but not different between each groups. In contrast to early postnatal rats, similar levels of LFS-induced LTD were obtained in all slices without or with ZD7288, L-NAME and ZD7288+L-NAME in adult rats.
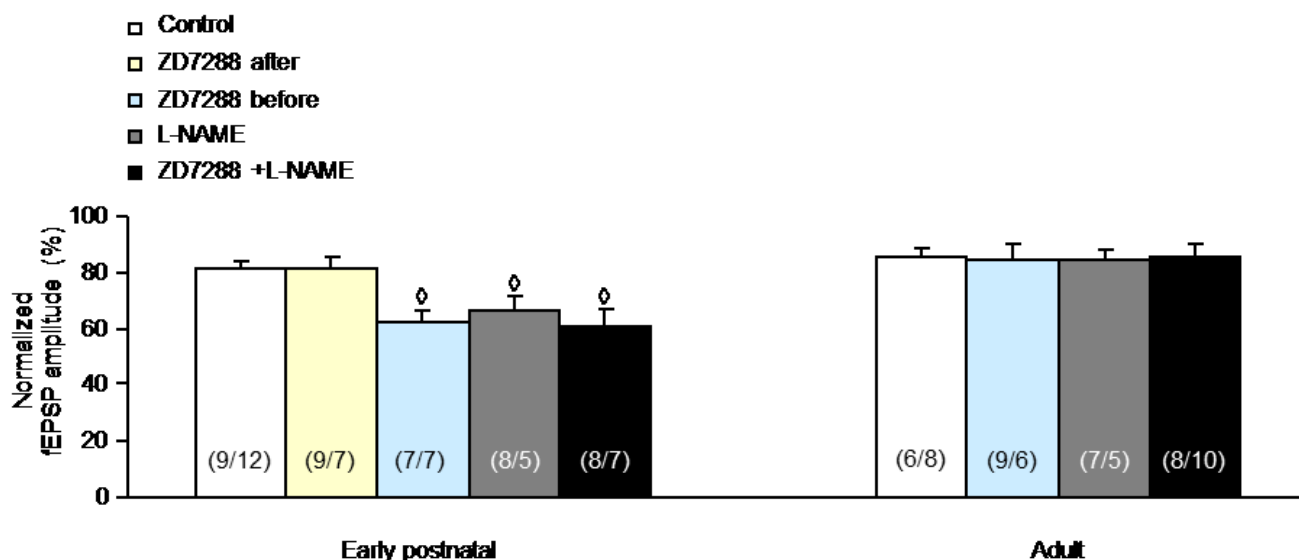
Figure 26: Comparison of LTD levels in different experimental conditions

Bar graphs summarize fEPSP amplitudes in different conditions: control (white), ZD7288 after (yellow), ZD7288 before (blue), L-NAME (gray), and ZD7288+L-NAME (black). The number of slices is given in parentheses (number of LFS-treated slices/number of non-LFS-treated slices). Note that, in early postnatal rats, LTD was significantly enhanced in similar degree in all groups when slices were perfused with ACSF containing ZD7288 (before LSF), L-NAME and ZD7288+L-NAME. In contrast to early postnatal rats, similar levels of LFS-induced LTD were obtained in all slices without or with ZD7288, L-NAME and ZD7288+L-NAME in adult rats.

4. Discussion

The role of HCN channels on synaptic plasticity is still not well known. Particularly the role of presynaptic HCN channels on MPP-LTD is not entirely clear. The major findings of the present study are as followings:

(1) HCN channel blocker ZD7288 causes a strong reduction of fEPSP amplitudes in MPP-granular cell synapses in both immature and adult tissues, but an increase of the paired-pulse ratio (PPR) only in immature synapses.

(2) Low-frequency stimulation (LFS) delivered to MPP resulted in LTD which was significantly enhanced by ZD7288 in the early postnatal age, but not in adult animals.

(3) LFS-induced LTD in MPP–granular cell synapses of both adult and early postnatal rats is NMDA receptor dependent.

(4) LFS delivered to MPP resulted in LTD which was significantly enhanced following application of NOS inhibitor L-NAME during the early postnatal age, but not in adult animals.

(5) LFS-induced LTD in MPP–granular cell synapses was also enhanced by co-application of L-NAME and ZD7288 in the early postnatal age, but the amount of LTD was not statistically different from the LTD obtained by the application of either of these compounds.

Taken together these findings, it is suggested that presynaptic HCN channel activation during neuronal activity may compromise the propensity of LTD obtained at these synapses.

4.1. Electrophysiological characterization of MPP–granular cell synapses

Information flows into the hippocampus mainly by the perforant path (PP) which targets neurons in the DG and in the CA1-3 regions. The axonal tracts that form the PP split into two anatomically and functionally distinct pathways, the MPP and the LPP. The MPP and the LPP, which travel along the middle and the outer third of stratum lacunosum-moleculare, respectively, and target different sections of the granule cell dendritic tree (Hjorthsi and Jeune, 1972;Sewards and Sewards, 2003;Steward, 1976;Witter, 1993). If electrodes were correctly positioned, we get paired-pulse depression in MPP-granular cell synapses (Dietrich et al., 1997;Kilbride et al., 1998) with a double-pulse stimulation protocol (40 ms interpulse interval), and paired-pulse facilitation in the LPP-DG synapses. However, an important pitfall in recording MPP-evoked fEPSPs is the potential contamination by field potentials following stimulation of the adjacent fiber tract—the lateral perforant path (LPP). The propensity of LTD to be obtained in the middle molecular layer may actually vary with the degree of contamination by LPP stimulation. Therefore, we analyzed the paired-pulse ratio (PPR) in all experimental groups at the beginning of the experiment, and we found no significant differences in the PPR between all groups (on average 76%), thus indicating a negligible contamination by LPP-evoked field potentials. In addition, gabazine (1 µM) was added to the ACSF in order to reduce contaminations by stimulation of local GABAergic interneuronal circuits (Houser, 2007).

4.2. Presynaptic HCN channels facilitate synaptic transmission in MPP–granular cell synapses by glutamate release

Previous reports have suggested that HCN channels are present at excitatory presynaptic terminals and may modulate transmitter release in the chick ciliary ganglion (Fletcher and Chiappinelli, 1992), the crayfish neuromuscular junction (Beaumont and Zucker, 2000), the rat calyx of Held synapse (Cuttle et al., 2001), and in the hippocampus (Bender et al., 2007), although HCN channels are both pre-and post-synaptically expressed in the IC and hippocampus (Notomi and Shigemoto, 2004).

We have shown that basal synaptic transmission is modulated by HCN channels at MPP-DG synapses. Blockade of HCN channels by ZD7288 caused a time-dependent decrease in fEPSP amplitude in both age groups, but accompanied by an increase in the PPR in postnatal but not adult rats indicating that pharmacological inhibition of HCN channels in postnatal tissue enhances glutamatergic synaptic transmission. The explanation of mechanisms mediated by ZD7288 in synaptic function may be confounded by other effects such as its action on glutamate receptors (Chen, 2004;Tokay et al., 2009). While LTD was found to be NMDA receptor dependent in both age groups, HCN channels are predominantly expressed on MPP axon terminals at early postnatal ages, but this presynaptic location is lost during

development (Bender et al., 2007;Tokay et al., 2009). Albeit postsynaptic expression of HCN channels on granule cell dendrites cannot entirely be excluded, there were no differences between slices from early postnatal and adult animals (Bender et al., 2007). In the present study, we, in fact, found a significant increase of the paired-pulse ratio by HCN channel inhibition in early postnatal, but not in adult tissue, confirming a facilitating role of presynaptic HCN channels in transmitter release. However, as it has been suggested that ZD7288 depresses synaptic transmission independently of affecting HCN channels (Chevaleyre and Castillo, 2002), it is possible that the observed effect of ZD7288 might be underestimated. This will be further clarified by using HCN knockout animals in our future studies.

Taken together, our results provide strong support for the involvement of presynaptic HCN channels in modulating MPP–granular cell synaptic transmission. Therefore, the differential effect of ZD7288 on LFS-induced LTD in these two age groups strongly supports the idea that presynaptic HCN channels contribute to the ZD7288-mediated LTD enhancement.

4.3. HCN channel activation modulates the induction but not the expression of LFS-induced LTD

As indicated by our finding that HCN channel constrain LFS-induced LTD in early postnatal but not in adult ones, which is compatible with Bender's work that HCN channels are predominantly expressed on MPP axon terminals at early postnatal ages but lost during maturation (Bender et al., 2007).

How can presynaptic HCN channels modulate LTD? In general, activity-dependent changes in synaptic strength may arise from both pre- and postsynaptic mechanisms. In hippocampal dendrites, it was proposed that HCN channels have at least two major effects, that is, (i) an active shunting conductance and (ii) a tonic depolarization leading to a reduced excitatory postsynaptic potential (EPSP) amplitude and a compromised temporal summation (Brager and Johnston, 2007;Fan et al., 2005;George et al., 2009;Magee, 1998;Magee, 1999;Poolos et al., 2002;Tsay et al., 2007). On the other side, presynaptic HCN channels have been suggested to increase the reliability of neurotransmitter release via exerting a tonic depolarization on the presynaptic membrane (Aponte et al., 2006). The underlying mechanisms may involve interaction with T-type Ca^{2+} channels as shown recently in axons terminating on entorhinal layer III pyramidal cells, where the HCN channels were found to influence Cav3.2 activity (Huang et al., 2011). Reducing presynaptic HCN activity could thus result in an altered frequency (Lupica et al., 2001;Southan et al., 2000) or failure rate (Debanne, 2004) of action potential-dependent transmitter release.

4.4. Postsynaptic NO production and presynaptic HCN channel activation compromise LFS-induced LTD at immature synapses

Nitric oxide (NO) is a free radical gas produced endogenously by a variety of mammalian cells, synthesized from arginine by nitric oxide synthases (NOSs). As a rapidly diffusible messenger molecule, NO has been implicated as a neuromodulator in synaptic transmission for two decades (Boehning and Snyder, 2003;Garthwaite, 2008;Snyder and Bredt, 1991). More specifically, there is indeed a large body of evidence supporting the role of NO in modulating synaptic transmission in the CA1 region of the hippocampus (Stanton et al., 2003;Zhang et al., 2006), reviewed in (Feil and Kleppisch, 2008), but the role of NO in the molecular layer of the dentate gyrus has attracted less attention. One study found that NO synthase inhibition blocked both LTP and LTD at these synapses (Wu et al., 1997). Despite this, the underlying mechanisms by which NO modulates synaptic transmission remain still an unraveled question. In our search for mechanism of presynaptic HCN channel modulation on MPP-LTD, we postulate that NO, as a signaling molecule produced in postsynapses and travels through the synaptic cleft to presynapses, modulates glutamate release via presynaptic HCN channels thus compromise LTD induction.

Under physiological conditions, NOSs, which comprise two isoforms in the neural tissue—the endothelial NOS (eNOS) and neuronal NOS (nNOS)—are responsible for the formation of NO as a signaling molecule. NOSs are calcium-dependent enzymes activated by Ca^{2+}–calmodulin complex under conditions of elevated intracellular Ca^{2+}concentrations by NMDAR activation at excitatory synapses (Christopherson et al., 1999;Makara et al., 2007;Prast and Philippu, 2001). This locally activation of NOSs enhances the production of NO in these synapses, which can freely cross cell membranes and is detectable only a few micrometers around its site of production (Namiki et al., 2005). Many of physiological effects of NO as a signaling molecule are mediated by activating specialized receptors NO-sensitive guanylate cyclases (NO-GCs) resulting in cGMP synthesis from GTP, a typical downstream effect of the NO retrograde signaling pathway (Feil and Kleppisch, 2008;Koesling et al., 2004;Mergia et al., 2009). There are two isoforms of NO-GC in the central nervous system, the more widely expressed NO-GC1, and NO-GC2 (Mergia et al., 2003). However, no differences have been detected between the isoforms in catalytic or regulatory properties (Russwurm et al., 1998).

The NO-induced the activation of NO-GCs and production of cGMP may alter the probability of vesicular release depending on the type of synaptic terminal and brain region(Garthwaite, 2008). The rodent hippocampus was found to express cGMP-producing NO-GCs (Koesling et al., 2004;Teunissen et al., 2001), and the expression of NOSs and NO-GCs was detected during the early postnatal days (Chung et al., 2004;Giuili et al., 1994). Synaptic distribution of these proteins indicated that NOSs are postsynaptically present in glutamatergic and GABAergic synapses, whereas the NO-GC is expressed in glutamatergic and GABAergic axon terminals (Cserep et al., 2011), suggesting that NO signaling is likely modulate transmitter release in these

synapses. In supporting these findings, measurements of long-term potentiation (LTP) in the hippocampus indicated that both NO-GC isoforms are required for LTP, as LTP was abolished in mice lacking either NO-GC1 or NO-GC2 (Taqatqeh et al., 2009). More recently, Neitz and colleagues found reductions in glutamate release in hippocampal synapses in the NO-GC1 KO mice (but not in NO-GC2 KO mice), and this was mimicked in wild-type (WT) mice upon pharmacological inhibition of NO∕cGMP signaling (Neitz et al., 2011). Interestingly, they also found that glutamate release was reduced by blockade of HCN channels in WT mice but not affected in NO-GC1 KO mice, suggesting that HCN channels are involved in the execution of cGMP effects (Neitz et al., 2011). In addition to this, it has been demonstrated that HCN channels are expressed in MPP terminals of early postnatal rats (Bender et al., 2007), and the activation of both NO signaling and HCN channels may modulate transmitter release (Garthwaite, 2008;Tokay et al., 2009).

In accordance with these findings, in the present study, we showed that exogenously application of blockers of either NO signaling pathways or HCN channels could induce fEPSP reduction concomitant with an enhancement of PPR in MPP-dentate gyrus synapses during of the early postnatal period, but not in adult rats, suggesting that both NO and HCN channel pathways are likely mediated by the modulation of presynaptic transmitter release in early postnatal animals. Finally, by pharmacological blockade of both NO pathways and HCN channels simultaneously, we found no additive reduction of transmitter release in these synapses, suggesting that the HCN channel and NO share the same pathways in the modulation of synaptic transmission. Based on our results together with findings from others, we propose that retrograde NO signaling pathways may alter the efficiency of glutamatergic synaptic transmission and LTD induction by modulating presynaptic HCN channel function via cGMP.

As a summary, according to results obtained in this study, I propose that, repetitive low frequency stimulation of the medial perforant path-granule cell synapse results in activation of NMDAs and a local increase in postsynaptic free Ca^{2+}. This Ca^{2+} then binds to calmodulin (CaM), and the Ca^{2+}–CaM complex has both direct and indirect actions on NOS activity. Ca^{2+}–CaM binds to NOS, resulting in an acute increase in NO production, as well as stimulating the protein phosphatase calcineurin, which in turn dephosphorylates NOS and increases its activity. The activation of Calcineurin by Ca^{2+}–CaM is long-lasting, maintaining NOS activation and NO production long after termination of the stimulus routine. NO activates NO-GCs to produce cGMP, and cGMP can activate cGMP-dependent protein kinase, and then activate HCN channels.
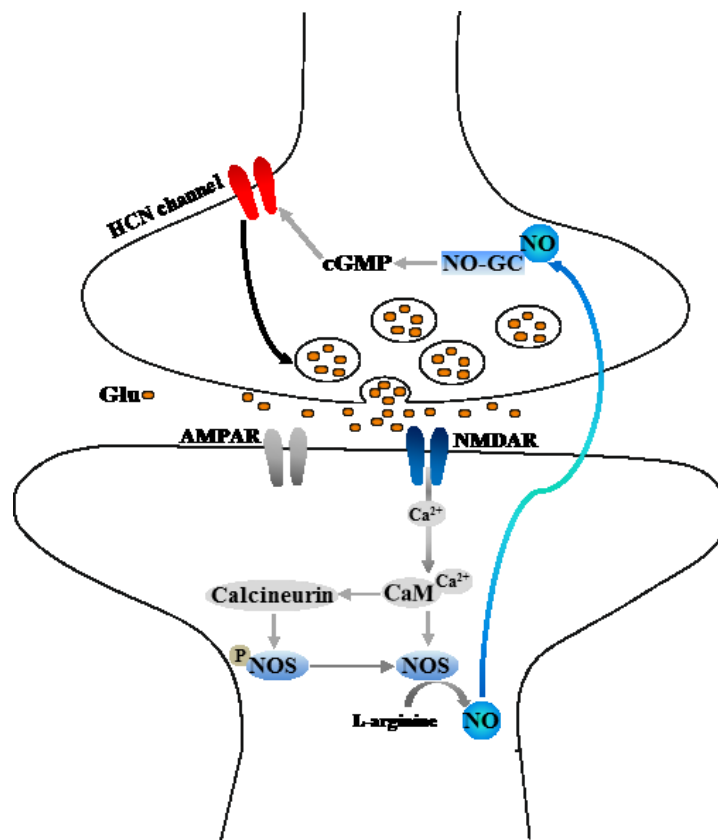
Figure 27: Retrograde NO signaling pathways compromise presynaptic HCN channel function in regulating MPP-LTD

LFS → enhancement of presynaptic glutamate release → depolarize DG granular cells → activation of NMDAR → enhanced Ca^{2+} influx → Ca^{2+} binding to CaM → enhanced NOS syntheses and calcineurin activation → constant production of NO → acting as a retrograde messenger NO traveling from the postsynaptic site to the presynaptic terminal → activation of presynaptic NO-GC → generation of second messenger cGMP within presynaptic terminal → presynaptic HCN channel activation → increase of glutamate release → enhanced synaptic transmission → less MPP-LTD. Denote letters: Glu, Glutamate; AMPAR, AMPA receptor; NMDAR, NMDA receptor; NO, nitric oxide; NOS, nitric oxide synthase; NO-GC, sensitive guanylate cyclases;

5. References

Reference List

Abraham WC (2003) How long will long-term potentiation last? Philosophical Transactions of the Royal Society B-Biological Sciences 358:735-744.

Abraham WC, Christie BR, Logan B, Lawlor P, Dragunow M (1994) Immediate-Early Gene-Expression Associated with the Persistence of Heterosynaptic Long-Term Depression in the Hippocampus. Proceedings of the National Academy of Sciences of the United States of America 91:10049-10053.

Aggleton JP, Brown MW (1999) Episodic memory, amnesia and the hippocampal-anterior thalamic axis. Behavioral and Brain Sciences 22:425-+.

Agmon A, Wells JE (2003) The role of the hyperpolarization-activated cationic current I-h in the timing of interictal bursts in the neonatal hippocampus. Journal of Neuroscience 23:3658-3668.

Aponte Y, Lien CC, Reisinger E, Jonas P (2006) Hyperpolarization-activated cation channels in fast-spiking interneurons of rat hippocampus. Journal of Physiology-London 574:229-243.

Bashir ZI, Collingridge GL (1994) An Investigation of Depotentiation of Long-Term Potentiation in the Ca1 Region of the Hippocampus. Experimental Brain Research 100:437-443.

Bear MF, Abraham WC (1996) Long-term depression in hippocampus. Annual Review of Neuroscience 19:437-462.

Beaumont V, Zucker RS (2000) Enhancement of synaptic transmission by cyclic AMP modulation of presynaptic I-h channels. Nature Neuroscience 3:133-141.

Bender RA, Brewster A, Santoro B, Ludwig A, Hofmann F, Biel M, Baram TZ (2001) Differential and age-dependent expression of hyperpolarization-activated, cyclic nucleotide-gated cation channel isoforms 1-4 suggests evolving roles in the developing rat hippocampus. Neuroscience 106:689-698.

Bender RA, Brewster AL, Baram TZ (2005) Neuronal activity influences the sub-cellular distribution of hyperpolarization-activated (HCN) cation channels in hippocampal neurons. Epilepsia 46:92.

Bender RA, Kirschstein T, Kretz O, Brewster AL, Richichi C, Rueschenschmidt C, Shigemoto R, Beck H, Frotscher M, Baram TZ (2007) Localization of HCN1 channels to presynaptic compartments: Novel plasticity that may contribute to hippocampal maturation. Journal of Neuroscience 27:4697-4706.

Biel M, Wahl-Schott C, Michalakis S, Zong X (2009) Hyperpolarization-Activated Cation Channels: From Genes to Function. Physiological Reviews 89:847-885.

Bliss TVP, Collingridge GL (1993) A Synaptic Model of Memory - Long-Term Potentiation in the Hippocampus. Nature 361:31-39.

Bliss TVP, Lomo T (1973) Long-Lasting Potentiation of Synaptic Transmission in Dentate Area of Anesthetized Rabbit Following Stimulation of Perforant Path. Journal of Physiology-London 232:331-356.

Boehning D, Snyder SH (2003) Novel neural modulators. Annual Review of Neuroscience 26:105-131.

Brager DH, Johnston D (2007) Plasticity of intrinsic excitability during long-term depression is mediated through mGluR-dependent changes in I-h in hippocampal CA1 pyramidal neurons. Journal of Neuroscience 27:13926-13937.

Brewster A, Bender RA, Chen YC, Dube C, Eghbal-Ahmadi M, Baram TZ (2002) Developmental febrile seizures modulate hippocampal gene expression of hyperpolarization-activated channels in an isoform- and cell-specific manner. Journal of Neuroscience 22:4591-4599.

Brewster AL, Bernard JA, Gall CM, Baram TZ (2005) Formation of heteromeric hyperpolarization-activated cyclic nucleotide-gated (HCN) channels in the hippocampus is regulated by developmental seizures. Neurobiology of Disease 19:200-207.

Brewster AL, Chen Y, Bender RA, Yeh A, Shigemoto R, Baram TZ (2007) Quantitative analysis and subcellular distribution of mRNA and protein expression of the hyperpolarization-activated cyclic nucleotide-gated channels throughout development in rat hippocampus. Cerebral Cortex 17:702-712.

Calabresi P, Maj R, Pisani A, Mercuri NB, Bernardi G (1992) Long-Term Synaptic Depression in the Striatum - Physiological and Pharmacological Characterization. Journal of Neuroscience 12:4224-4233.

Campanac E, Daoudal G, Ankri N, Debanne D (2008) Downregulation of dendritic I-h in CA1 pyramidal neurons after LTP. Journal of Neuroscience 28:8635-8643.

Carroll RC, Lissin DV, von Zastrow M, Nicoll RA, Malenka RC (1999) Rapid redistribution of glutamate receptors contributes to long-term depression in hippocampal cultures. Nature Neuroscience 2:454-460.

Cerbone A, Patacchioli FR, Sadile AG (1993) A Neurogenetic and Morphogenetic Approach to Hippocampal Functions Based on Individual-Differences and Neurobehavioral Covariations. Behavioural Brain Research 55:1-16.

Chen C (2004) ZD7288 inhibits postsynaptic glutamate receptor-mediated responses at hippocampal perforant path-granule cell synapses. European Journal of Neuroscience 19:643-649.

Chen S, Wang J, Siegelbaum SA (2001) Properties of hyperpolarization-activated pacemaker current defined by coassembly of HCN1 and HCN2 subunits and

basal modulation by cyclic nucleotide. The Journal of general physiology 117:491-504.

Chevaleyre V, Castillo PE (2002) Assessing the role of Ih channels in synaptic transmission and mossy fiber LTP. Proceedings of the National Academy of Sciences of the United States of America 99:9538-9543.

Christie BR, Magee JC, Johnston D (1996) The role of dendritic action potentials and Ca2+ influx in the induction of homosynaptic long-term depression in hippocampal CA1 pyramidal neurons. Learning & Memory 3:160-169.

Christopherson KS, Hillier BJ, Lim WA, Bredt DS (1999) PSD-95 assembles a ternary complex with the N-methyl-D-aspartic acid receptor and a bivalent neuronal NO synthase PDZ domain. Journal of Biological Chemistry 274:27467-27473.

Chung YH, Kim YS, Lee WB (2004) Distribution of neuronal nitric oxide synthase-immunoreactive neurons in the cerebral cortex and hippocampus during postnatal development. Journal of Molecular Histology 35:765-770.

Collingridge GL, Kehl SJ, Mclennan H (1983) Excitatory Amino-Acids in Synaptic Transmission in the Schaffer Collateral Commissural Pathway of the Rat Hippocampus. Journal of Physiology-London 334:33-46.

Crowder JM, Croucher MJ, Bradford HF, Collins JF (1987) Excitatory Amino-Acid Receptors and Depolarization-Induced Ca-2+ Influx Into Hippocampal Slices. Journal of Neurochemistry 48:1917-1924.

Cserep C, Szonyi A, Veres JM, Nemeth B, Szabadits E, de Vente J, Hajos N, Freund TF, Nyiri G (2011) Nitric Oxide Signaling Modulates Synaptic Transmission during Early Postnatal Development. Cerebral Cortex 21:2065-2074.

Cull-Candy S, Brickley S, Farrant M (2001) NMDA receptor subunits: diversity, development and disease. Current Opinion in Neurobiology 11:327-335.

Cummings JA, Mulkey RM, Nicoll RA, Malenka RC (1996) Ca2+ signaling requirements for long-term depression in the hippocampus. Neuron 16:825-833.

Cuttle MF, Rusznak Z, Wong AYC, Owens S, Forsythe ID (2001) Modulation of a presynaptic hyperpolarization-activated cationic current (I-h) at an excitatory synaptic terminal in the rat auditory brainstem. Journal of Physiology-London 534:733-744.

Debanne D (2004) Information processing in the axon. Nature Reviews Neuroscience 5:304-316.

Dietrich D, Beck H, Kral T, Clusmann H, Elger CE, Schramm J (1997) Metabotropic glutamate receptors modulate synaptic transmission in the perforant path: pharmacology and localization of two distinct receptors. Brain Research 767:220-227.

Dingledine R, Borges K, Bowie D, Traynelis SF (1999) The glutamate receptor ion channels. Pharmacological Reviews 51:7-61.

Dolorfo CL, Amaral DG (1998) Entorhinal cortex of the rat: Topographic organization of the cells of origin of the perforant path projection to the dentate gyrus. Journal of Comparative Neurology 398:25-48.

Doyere V, Burette F, Redinidelnegro C, Laroche S (1993) Long-Term Potentiation of Hippocampal Afferents and Efferents to Prefrontal Cortex - Implications for Associative Learning. Neuropsychologia 31:1031-1053.

Doyere V, Srebro B, Laroche S (1997) Heterosynaptic LTD and depotentiation in the medial perforant path of the dentate gyrus in the freely moving rat. Journal of Neurophysiology 77:571-578.

Dudek SM, Bear MF (1992) Homosynaptic Long-Term Depression in Area Ca1 of Hippocampus and Effects of N-Methyl-D-Aspartate Receptor Blockade. Proceedings of the National Academy of Sciences of the United States of America 89:4363-4367.

Ehlers MD (2000) Reinsertion or degradation of AMPA receptors determined by activity-dependent endocytic sorting. Neuron 28:511-525.

Enoki R, Hu Yl, Hamilton D, Fine A (2009) Expression of Long-Term Plasticity at Individual Synapses in Hippocampus Is Graded, Bidirectional, and Mainly Presynaptic: Optical Quantal Analysis. Neuron 62:242-253.

Fan Y, Fricker D, Brager DH, Chen XX, Lu HC, Chitwood RA, Johnston D (2005) Activity-dependent decrease of excitability in rat hippocampal neurons through increases in I-h. Nature Neuroscience 8:1542-1551.

Feil R, Kleppisch T (2008) NO/cGMP-dependent modulation of synaptic transmission. Handbook of experimental pharmacology529-560.

Feinmark SJ, Begum R, Tsvetkov E, Goussakov I, Funk CD, Siegelbaum SA, Bolshakov VY (2003) 12-lipoxygenase metabolites of arachidonic acid mediate metabotropic glutamate receptor-dependent long-term depression at hippocampal CA3-CA1 synapses. Journal of Neuroscience 23:11427-11435.

Fletcher GH, Chiappinelli VA (1992) An Inward Rectifier Is Present in Presynaptic Nerve-Terminals in the Chick Ciliary Ganglion. Brain Research 575:103-112.

Fujii S, Saito K, Miyakawa H, Ito K, Kato H (1991) Reversal of Long-Term Potentiation (Depotentiation) Induced by Tetanus Stimulation of the Input to Ca1 Neurons of Guinea-Pig Hippocampal Slices. Brain Research 555:112-122.

Garthwaite J (2008) Concepts of neural nitric oxide-mediated transmission. European Journal of Neuroscience 27:2783-2802.

Gauss R, Seifert R (2000) Pacemaker oscillations in heart and brain: a key role for hyperpolarization-activated cation channels. Chronobiology International 17:453-469.

George MS, Abbott L, Siegelbaum SA (2009) HCN hyperpolarization-activated cation channels inhibit EPSPs by interactions with M-type K+ channels. Nature Neuroscience 12:577-584.

Giuili G, Luzi A, Poyard M, Guellaen G (1994) Expression of mouse brain soluble guanylyl cyclase and NO synthase during ontogeny. Brain research Developmental brain research 81:269-283.

Hjorthsi A, Jeune B (1972) Origin and Termination of Hippocampal Perforant Path in Rat Studied by Silver Impregnation. Journal of Comparative Neurology 144:215-&.

Hollmann M, Heinemann S (1994) Cloned Glutamate Receptors. Annual Review of Neuroscience 17:31-108.

Hollmann M, Osheagreenfield A, Rogers SW, Heinemann S (1989) Cloning by Functional Expression of A Member of the Glutamate Receptor Family. Nature 342:643-648.

Houser CR (2007) Interneurons of the dentate gyrus: an overview of cell types, terminal fields and neurochemical identity. Dentate Gyrus: A Comphrehensive Guide to Structure, Function, and Clinical Implications 163:217-+.

Huang Z, Lujan R, Kadurin I, Uebele VN, Renger JJ, Dolphin AC, Shah MM (2011) Presynaptic HCN1 channels regulate Ca(V)3.2 activity and neurotransmission at select cortical synapses. Nature Neuroscience 14:478-U114.

Huang Z, Walker MC, Shah MM (2009) Loss of Dendritic HCN1 Subunits Enhances Cortical Excitability and Epileptogenesis. Journal of Neuroscience 29:10979-10988.

Johnson JW, Ascher P (1990) Voltage-Dependent Block by Intracellular Mg-2+ of N-Methyl-D-Aspartate-Activated Channels. Biophysical Journal 57:1085-1090.

Kemp A, Manahan-Vaughan D (2007) Hippocampal long-term depression: master or minion in declarative memory processes? Trends in Neurosciences 30:111-118.

Kilbride J, Huang LQ, Rowan MJ, Anwyl R (1998) Presynaptic inhibitory action of the group II metabotropic glutamate receptor agonists, LY354740 and DCG-IV. European Journal of Pharmacology 356:149-157.

Kleckner NW, Dingledine R (1988) Requirement for Glycine in Activation of Nmda-Receptors Expressed in Xenopus Oocytes. Science 241:835-837.

Kobayashi M, Ohno M, Shibata S, Yamamoto T, Watanabe S (1997) Concurrent blockade of beta-adrenergic and muscarinic receptors suppresses synergistically long-term potentiation of population spikes in the rat hippocampal CA1 region. Brain Research 777:242-246.

Koesling D, Russwurm M, Mergia E, Mullershausen F, Friebe A (2004) Nitric oxide-sensitive guanylyl cyclase: structure and regulation. Neurochemistry International 45:813-819.

Laube B, Kuhse J, Betz H (1998) Evidence for a tetrameric structure of recombinant NMDA receptors. Journal of Neuroscience 18:2954-2961.

Lee HK, Barbarosie M, Kameyama K, Bear MF, Huganir RL (2000) Regulation of distinct AMPA receptor phosphorylation sites during bidirectional synaptic plasticity. Nature 405:955-959.

Lee HK, Kameyama K, Huganir RL, Bear MF (1998) NMDA induces long-term synaptic depression and dephosphorylation of the GluR1 subunit of AMPA receptors in hippocampus. Neuron 21:1151-1162.

Levy WB, Steward O (1979) Synapses As Associative Memory Elements in the Hippocampal-Formation. Brain Research 175:233-245.

Lodge D (2009) The history of the pharmacology and cloning of ionotropic glutamate receptors and the development of idiosyncratic nomenclature. Neuropharmacology 56:6-21.

Lomo T (2003) The discovery of long-term potentiation. Philosophical Transactions of the Royal Society of London Series B-Biological Sciences 358:617-620.

Lorincz A, Notomi T, Tamas G, Shigemoto R, Nusser Z (2002) Polarized and compartment-dependent distribution of HCN1 in pyramidal cell dendrites. Nature Neuroscience 5:1185-1193.

Ludwig A, Zong XG, Jeglitsch M, Hofmann F, Biel M (1998) A family of hyperpolarization-activated mammalian cation channels. Nature 393:587-591.

Lujan R, Albasanz JL, Shigemoto R, Juiz JM (2005) Preferential localization of the hyperpolarization-activated cyclic nucleotide-gated cation channel subunit HCN1 in basket cell terminals of the rat cerebellum. European Journal of Neuroscience 21:2073-2082.

Lupica CR, Bell JA, Hoffman AF, Watson PL (2001) Contribution of the hyperpolarization-activated current (I-h)to membrane potential and GABA release in hippocampal interneurons. Journal of Neurophysiology 86:261-268.

Lynch G, Larson J, Kelso S, Barrionuevo G, Schottler F (1983) Intracellular Injections of Egta Block Induction of Hippocampal Long-Term Potentiation. Nature 305:719-721.

Lynch GS, Dunwiddie T, Gribkoff V (1977) Heterosynaptic Depression - Postsynaptic Correlate of Long-Term Potentiation. Nature 266:737-739.

Magee JC (1998) Dendritic hyperpolarization-activated currents modify the integrative properties of hippocampal CA1 pyramidal neurons. Journal of Neuroscience 18:7613-7624.

Magee JC (1999) Dendritic I-h normalizes temporal summation in hippocampal CA1 neurons. Nature Neuroscience 2:508-514.

Makara JK, Katona I, Nyiri G, Nemeth B, Ledent C, Watanabe M, de Vente J, Freund TF, Hajos N (2007) Involvement of nitric oxide in depolarization-induced suppression of inhibition in hippocampal pyramidal cells during activation of cholinergic receptors. Journal of Neuroscience 27:10211-10222.

Malenka RC, Bear MF (2004) LTP and LTD: An embarrassment of riches. Neuron 44:5-21.

Malenka RC, Nicoll RA (1999) Neuroscience - Long-term potentiation - A decade of progress? Science 285:1870-1874.

Malinow R, Malenka RC (2002) AMPA receptor trafficking and synaptic plasticity. Annual Review of Neuroscience 25:103-126.

Mayer ML, Armstrong N (2004) Structure and function of glutamate receptor ion channels. Annual Review of Physiology 66:161-181.

Mccormick DA, Pape HC (1990) Noradrenergic and Serotonergic Modulation of A Hyperpolarization-Activated Cation Current in Thalamic Relay Neurons. Journal of Physiology-London 431:319-342.

Mcentee WJ, Crook TH (1993) Glutamate - Its Role in Learning, Memory, and the Aging Brain. Psychopharmacology 111:391-401.

Mellor J, Nicoll RA, Schmitz D (2002) Mediation of hippocampal mossy fiber long-term potentiation by presynaptic I-h channels. Science 295:143-147.

Mergia E, Russwurm M, Zoidl G, Koesling D (2003) Major occurrence of the new alpha(2)beta(1) isoform of NO-sensitive guanylyl cyclase in brain. Cellular Signalling 15:189-195.

Mergia E, Koesling D, Friebe A (2009) Genetic mouse models of the NO receptor 'soluble' guanylyl cyclases. Handbook of experimental pharmacology33-46.

Monteggia LM, Eisch AJ, Tang MD, Kaczmarek LK, Nestler EJ (2000a) Cloning and localization of the hyperpolarization-activated cyclic nucleotide-gated channel family in rat brain. Brain research Molecular brain research 81:129-139.

Mulkey RM, Endo S, Shenolikar S, Malenka RC (1994) Involvement of A Calcineurin/Inhibitor-1 Phosphatase Cascade in Hippocampal Long-Term Depression. Nature 369:486-488.

Mulkey RM, Herron CE, Malenka RC (1993) An Essential Role for Protein Phosphatases in Hippocampal Long-Term Depression. Science 261:1051-1055.

Mulkey RM, Malenka RC (1992) Mechanisms Underlying Induction of Homosynaptic Long-Term Depression in Area Ca1 of the Hippocampus. Neuron 9:967-975.

Mumby DG, Astur RS, Weisend MP, Sutherland RJ (1999) Retrograde amnesia and selective damage to the hippocampal formation: memory for places and object discriminations. Behavioural Brain Research 106:97-107.

Namiki S, Kakizawa S, Hirose K, Iino M (2005) NO signalling decodes frequency of neuronal activity and generates synapse-specific plasticity in mouse cerebellum. Journal of Physiology-London 566:849-863.

Neitz A, Mergia E, Eysel UT, Koesling D, Mittmann T (2011) Presynaptic nitric oxide/cGMP facilitates glutamate release via hyperpolarization-activated cyclic nucleotide-gated channels in the hippocampus. European Journal of Neuroscience 33:1611-1621.

Nolan MF, Malleret G, Dudman JT, Buhl DL, Santoro B, Gibbs E, Vronskaya S, Buzsaki G, Siegelbaum SA, Kandel ER, Morozov A (2004) A behavioral role for dendritic integration: HCN1 channels constrain spatial inputs to distal dendrites memory and plasticity at of CA1 pyramidal neurons. Cell 119:719-732.

Noma A, Irisawa H (1976) Membrane Currents in Rabbit Sinoatrial Node Cell As Studied by Double Microelectrode Method. Pflugers Archiv-European Journal of Physiology 364:45-52.

Notomi T, Shigemoto R (2004) Immunohistochemical localization of I-h channel subunits, HCN1-4, in the rat brain. Journal of Comparative Neurology 471:241-276.

O'Dell TJ, Kandel ER (1994) Low-frequency stimulation erases LTP through an NMDA receptor-mediated activation of protein phosphatases. Learning & memory (Cold Spring Harbor, N Y) 1:129-139.

Oliet SHR, Malenka RC, Nicoll RA (1997) Two distinct forms of long-term depression coexist in CA1 hippocampal pyramidal cells. Neuron 18:969-982.

Omara SM, Rowan MJ, Anwyl R (1995a) Dantrolene Inhibits Long-Term Depression and Depotentiation of Synaptic Transmission in the Rat Dentate Gyrus. Neuroscience 68:621-624.

Omara SM, Rowan MJ, Anwyl R (1995b) Metabotropic Glutamate Receptor-Induced Homosynaptic Long-Term Depression and Depotentiation in the Dentate Gyrus of the Rat Hippocampus In-Vitro. Neuropharmacology 34:983-989.

Paoletti P, Neyton J (2007) NMDA receptor subunits: function and pharmacology. Current Opinion in Pharmacology 7:39-47.

Pape HC (1996) Queer current and pacemaker: The hyperpolarization-activated cation current in neurons. Annual Review of Physiology 58:299-327.

Peterson BS, Choi HA, Hao X, Amat JA, Zhu H, Whiteman R, Liu J, Xu D, Bansal R (2007) Morphologic features of the amygdala and hippocampus in children and adults with Tourette syndrome. Archives of General Psychiatry 64:1281-1291.

Poolos NP, Migliore M, Johnston D (2002) Pharmacological upregulation of h-channels reduces the excitability of pyramidal neuron dendrites. Nature Neuroscience 5:767-774.

Prast H, Philippu A (2001) Nitric oxide as modulator of neuronal function. Progress in Neurobiology 64:51-68.

Reilly CE (2001) Hippocampus selectively supports episodic memory retrieval. Journal of Neurology 248:1014-1015.

Robinson RB (2003) Hyperpolarization-activated cation currents: From molecules to physiological function. Annual Review of Physiology 65:453-480.

Russwurm M, Behrends S, Harteneck C, Koesling D (1998) Functional properties of a naturally occurring isoform of soluble guanylyl cyclase. Biochemical Journal 335:125-130.

Santoro B, Baram TZ (2003) The multiple personalities of h-channels. Trends in Neurosciences 26:550-554.

Santoro B, Chen S, Luthi A, Pavlidis P, Shumyatsky GP, Tibbs GR, Siegelbaum SA (2000) Molecular and functional heterogeneity of hyperpolarization-activated pacemaker channels in the mouse CNS. Journal of Neuroscience 20:5264-5275.

Santoro B, Tibbs GR (1999) The HCN gene family: Molecular basis of the hyperpolarization-activated pacemaker channels.

Scoville WB, Milner B (1957) Loss of Recent Memory After Bilateral Hippocampal Lesions. Journal of Neurology Neurosurgery and Psychiatry 20:11-21.

Sewards TV, Sewards MA (2003) Input and output stations of the entorhinal cortex: superficial vs. deep layers or lateral vs. medial divisions? Brain Research Reviews 42:243-251.

Simeone TA, Rho JM, Baram TZ (2005) Single channel properties of hyperpolarization-activated cation currents in acutely dissociated rat hippocampal neurones. Journal of Physiology-London 568:371-380.

Snyder SH, Bredt DS (1991) Nitric-Oxide As A Neuronal Messenger. Trends in Pharmacological Sciences 12:125-128.

Southan AP, Morris NP, Stephens GJ, Robertson B (2000) Hyperpolarization-activated currents in presynaptic terminals of mouse cerebellar basket cells. Journal of Physiology-London 526:91-97.

Stanton PK, Winterer J, Bailey CP, Kyrozis A, Raginov I, Laube G, Veh RW, Nguyen CQ, Muller W (2003) Long-term depression of presynaptic release from the readily releasable vesicle pool induced by NMDA receptor-dependent retrograde nitric oxide. Journal of Neuroscience 23:5936-5944.

Staubli U, Lynch G (1987) Stable Hippocampal Long-Term Potentiation Elicited by Theta-Pattern Stimulation. Brain Research 435:227-234.

Staubli U, Lynch G (1990) Stable Depression of Potentiated Synaptic Responses in the Hippocampus with 1-5 Hz Stimulation. Brain Research 513:113-118.

Steward O (1976) Topographic Organization of Projections from Entorhinal Area to Hippocampal Formation of Rat. Journal of Comparative Neurology 167:285-314.

Surges R, Brewster AL, Bender RA, Beck H, Feuerstein TJ, Baram TZ (2006) Regulated expression of HCN channels and cAMP levels shape the properties of the h current in developing rat hippocampus. European Journal of Neuroscience 24:94-104.

Taqatqeh F, Mergia E, Neitz A, Eysel UT, Koesling D, Mittmann T (2009) More than a Retrograde Messenger: Nitric Oxide Needs Two cGMP Pathways to Induce Hippocampal Long-Term Potentiation. Journal of Neuroscience 29:9344-9350.

Teunissen C, Steinbusch H, Markerink-van Ittersum M, Koesling D, de Vente J (2001) Presence of soluble and particulate guanylyl cyclase in the same hippocampal astrocytes. Brain Research 891:206-212.

Tokay T, Rohde M, Krabbe S, Rehberg M, Bender RA, Koehling R, Kirschstein T (2009) HCN1 channels constrain DHPG-induced LTD at hippocampal Schaffer collateral-CA1 synapses. Learning & Memory 16:769-776.

Tsay D, Dudman JT, Siegelbaum SA (2007) HCN1 channels constrain synaptically evoked Ca2+ spikes in distal dendrites of CA1 pyramidal neurons. Neuron 56:1076-1089.

Vasilyev DV, Barish ME (2000) Integrin regulation of I-h expression in neonatal hippocampal pyramidal neurons. Neurophysiology 32:136.

Vasilyev DV, Barish ME (2002) Postnatal development of the hyperpolarization-activated excitatory current I-h in mouse hippocampal pyramidal neurons. Journal of Neuroscience 22:8992-9004.

Wang M, Ramos BP, Paspalas CD, Shu Y, Simen A, Duque A, Vijayraghavan S, Brennan A, Dudley A, Nou E, Mazer JA, McCormick DA, Arnsten AF (2007) alpha 2A-adrenoceptors strengthen working memory networks by inhibiting cAMP-HCN channel signaling in prefrontal cortex. Cell 129:397-410.

Wang SJ, Gean PW (1999) Long-term depression of excitatory synaptic transmission in the rat amygdala. Journal of Neuroscience 19:10656-10663.

Wang Y, Rowan MJ, Anwyl R (1997) Induction of LTD in the dentate gyrus in vitro is NMDA receptor independent, but dependent on Ca2+ influx via low-voltage-activated Ca2+ channels and release of Ca2+ from intracellular stores. Journal of Neurophysiology 77:812-825.

Wilkars W, Liu Z, Lewis AS, Stoub TR, Ramos EM, Brandt N, Nicholson DA, Chetkovich DM, Bender RA (2012) Regulation of axonal HCN1 trafficking in

perforant path involves expression of specific TRIP8b isoforms. PloS one 7:e32181.

Williams SR, Stuart GJ (2000) Site independence of EPSP time course is mediated by dendritic I-h in neocortical pyramidal neurons. Journal of Neurophysiology 83:3177-3182.

Witter MP (1993) Organization of the Entorhinal Hippocampal System - A Review of Current Anatomical Data. Hippocampus 3:33-44.

Wolosker H (2006) D-serine regulation of NMDA receptor activity. Science's STKE : signal transduction knowledge environment 2006:e41.

Wu J, Wang Y, Rowan MJ, Anwyl R (1997) Evidence for involvement of the neuronal isoform of nitric oxide synthase during induction of long-term potentiation and long-term depression in the rat dentate gyrus in vitro. Neuroscience 78:393-398.

Zhang XI, Zhou Zy, Winterer J, Mueller W, Stanton PK (2006) NMDA-dependent, but not group I metabotropic glutamate receptor-dependent, long-term depression at schaffer collateral-CA1 synapses is associated with long-term reduction of release from the rapidly recycling presynaptic vesicle pool. Journal of Neuroscience 26:10270-10280.

Ziakopoulos Z, Tillett CW, Brown MW, Bashir ZI (1999) Input- and layer-dependent synaptic plasticity in the rat perirhinal cortex in vitro. Neuroscience 92:459-472.

CURRICULUM VITAE

PERSONAL INFORMATION

Surname / First name:	Badel / Gulshat (Guli / Xiati)
Gender:	Female
Date and place of birth:	05.05.1985, Xinjiang, China
Nationality:	Chinese
Address:	University of Rostock
	Medical Faculty
	Gertrudenstrasse 9
	18057 Rostock
	Germany
Telephone:	004917667465821
E-mails:	xiati.guli@uni-rostock.de

EDUCATION

12 / 2010 – Present:	Ph.D student at University of Rostock
	Rostock, Germany
09 / 2005 – 07 / 2010:	B.Sc +M.S in Clinical Medicine, Fudan University
	Shanghai, China
09 / 2001 – 07 / 2005:	Qibao High School
	Shanghai, China
09 / 1998 – 07 / 2001:	Jemsar Junior High School
	Xinjiang, China

WORK EXPERIENCE

01 / 2010 – 07 / 2010:	Zhongshan Hospital
	Shanghai, China
11 / 2009 – 12 / 2009:	Neuroanatomy Research Group, Institute of Anatomy
	Fudan University, Shanghai, China
08 / 2009 – 10 / 2009:	Neurology Department, Zhongshan Hospital
	Shanghai, China

06 / 2009 – 07 / 2009:   Eye Ear Nose and Throat Hospital
Shanghai, China

PUBLICATION

Guli X, Tokay T, Guli X, Rohde M, Bender RA, Köhling R, Kirschstein T. ZD7288 enhances long-term depression at early postnatal medial perforant path-granule cell synapses. Neural Plast. 2012:237913

Till Janusz Würdemann, Mchristian Bien, Maxi Kersten, Marco Rohde, Tursonjan Tokay, **Xiati Guli,** Rüdiger Köhling und Timo Kirschstein. Stereotactic injection of cerebrospinal fluid from anti-NMDA receptor encephalitis into rat dentate gyrus impairs NMDA receptor function. Submitted to Neural biology disease (in Preparation)

SCIENTIFIC CONGRESS

Xiati G., Tokay T., Rohde M., Bender R., Köhling R., Kirschstein T. HCN channels constrain long-term depression at medial perforant path–granule cell synapses of early postnatal rats. 91st Annual Meeting of German Physiological Society March 22-25, 2012, Dresden, Germany.

M. Rohde, **X. Guli**, R. Köhling, T. Kirschstein.. 92nd German Physiologial Society (DPG) Annual Meeting, March 02-05, 2013, Heidelberg, Germany.

PERSONAL SKILLS AND COMPETENCES

Language:	Chinese (Fluent)
	English (IELTS score: 6.5)
	Kazakh (mother language)
Computer skills and competences:	Proficient in working with Microsoft Excel, Word, PowerPoint, VB.
	Familiar with different operating systems such as Windows
Organization and management capacity:	Chef of Student Union at Fundan University

Statement of independence

I hereby declare that this thesis is my own original work.

All the literature I used is properly quoted and is listed in Reference.

I completed all my work independently.

Rostock, 12.03.2013

Badel Gulshat (Guli Xiati)

Acknowledgment

This dissertation would not have been possible without the guidance and the help of several individuals who contributed and extended their valuable assistance in the preparation and completion of this study.

Foremost, my sincere thanks go to the Director of the Institute Professor Dr. Rüdiger Köhling for the continuous support of my Ph.D study and research. I really appreciate his vast knowledge, talent and skills in many areas (e.g., epilepsy, aging, hypoxic damage).

I would like to express my sincere gratitude to PD. Dr. Timo Kirschstein for his expertise, patience and enthusiasm, for being an excellent supervisor and for giving me an opportunity to undertake this project in the Institute of Physiology at Rostock University. His guidance helped me in all the time of research and writing of this thesis. I could not have imagined having a better advisor and mentor for my Ph.D study.

A very special thanks goes out to Dr. Tursonjan Tokay, without his motivation and encouragement I would not have considered a graduate career in sicentific research. Dr. Tokay is the one who truly made a difference in my life. It was under his suggestion that I became interested in Neuroscience. He provided me with direction, technical support and later became more a friend than a supervisor. Thanks to his support, understanding and kindness. I doubt that I will ever be able to convey my appreciation fully, but I owe him my eternal gratitude.

I must acknowledge Mr. Marco Rohde for his teaching skills, debates, exchanges of knowledge, and valuable suggestions throughout my graduate program.

Appreciation also goes out to Dr. Lorenz Müller and Dr. Steffen Müller for their help and advice at times of critical need.

Thanks to Dr. Mewes Hartmut for his kind support of my work.

I would also like to thank Dr. Roland Bender from Institute of Neuroanatomy at the University of Hamburg for the assistance in my research project.

I would like to appreciate the secretary of the institute Ms. Mandy Riedel for her friendship and kind help during my study in the institute.

I also appreciate Memmener Bernd and Hanka Schmidt for excellent technical assistance and animal care.

This research would not have been possible without support by a Grant from the German Research Council (KI 1283/3-1) and express my sincere gratitude to the agency.

Finally, I would also like to thank my parents and brothers for their love, support and encouragement they gave me through my entire life.